RARE-ELEMENT-ENRICHED PEGMATITES
IN CENTRAL NEWFOUNDLAND

Z. Magyarosi
Mineral Development Section

ABSTRACT

Anomalously high fluorine concentrations in till samples (up to 948 ppm) were recently identified in the Snowshoe Pond and surrounding areas in central Newfoundland. The area lies within the Meelpaeg Subzone of the Gander Zone and comprises metasedimentary rocks of the Spruce Brook Formation intruded by granitoid rocks of Ordovician to Devonian age. Anomalous fluorine values are associated with pegmatite dykes, the Snowshoe Pond Granite and, locally, the metasedimentary rocks of the Spruce Brook Formation.

Pegmatite dykes are composed of quartz, K-feldspar, plagioclase, muscovite, garnet, biotite, apatite and trace amounts of zircon, monazite, xenotime, magnetite, hematite, pyrite, gahnite ($ZnAl_2O_4$), tourmaline, "coltan" (solid solution between columbite and tantalite) and beryl. The main fluorine-bearing minerals are muscovite and apatite; the latter occurring in amounts up to 5%. Whereas the pegmatites show depletion in rare-earth elements, they are richer in MnO, Rb, U, P_2O_5, Be, Cs, Ta and Li and poorer in Zr and Th than the other granites. The pegmatites represent the most fractionated granitic intrusive phase in the study area, as suggested by their Nb and Ta contents. They are syn-collisional, Li–F granites.

The pegmatites are classed as Li–Cs–Ta-type (LCT), or rare-element-enriched pegmatites that are well known for their association with economic concentrations of rare elements in the Superior Province in Ontario and Manitoba. The geological setting of the pegmatites in the study area is similar to the setting of the Superior Province pegmatites, in that they are commonly located along a major geological boundary and are, locally, hosted in metasedimentary rocks. The grade of metamorphism is greenschist to amphibolite facies, although locally higher; and the host rocks, including the Snowshoe Pond Granite and rocks of the Spruce Brook Formation, display signs of metasomatic alteration, characteristic of rare-element pegmatites.

Rare-element pegmatites crystallize from the residual melt of an evolved parent granite magma that migrates into the host rocks. The parent granite is termed 'fertile' and consists of several intrusive phases. The whole-rock chemical composition, mineralogy and texture of the pegmatites are typical of the pegmatitic leucogranite phase of a fertile granite, except for their Nb/Ta ratios, which are slightly higher in central Newfoundland. The presence of a fertile parent granite was not confirmed in this study, but the best candidate would be similar in composition to the Wolf Mountain Granite, which is the only sufficiently fractionated, posttectonic granitic intrusion in the area. Based on outcrop distribution, it appears the Wolf Mountain Granite is too distant (> 10 km) to be the parent granite of the pegmatites. However, a chemically similar intrusion may occur at depth beneath the pegmatite dykes.

Further work should include exploration for additional pegmatite dykes and a potential fertile parent granite. Examination of chemical and mineralogical zoning, within potentially fertile granites and associated pegmatite dykes, is recommended to determine a fractionation trend. As the degree of fractionation in fertile granites is directly correlated with the economic potential of the pegmatites, definition of such trends could help in locating pegmatites that have the highest potential for economic rare-element mineralization.

High fluorine in till samples was successfully used to locate rare-element-enriched pegmatites in the Snowshoe Pond area, but more work is needed to assess their economic potential. Till sampling over rare-element mineralized rocks is recommended to assess the application of fluorine in till samples as indicators for economic quantities of rare-element mineralization.

INTRODUCTION

The purpose of this study is to complement the results of regional till samples from the Snowshoe Pond and surrounding areas in central Newfoundland that yielded anomalously high fluorine concentrations, up to 948 ppm (Figure 1; Smith *et al.*, 2009; Organ, 2014; Campbell *et al.*, 2017; Campbell, 2018, 2019). Fieldwork in 2019 attempted to identify the bedrock source of the fluorine anomalies and to investigate the potential of the bedrock source to host rare-element and/or fluorite mineralization. Sampling concentrated on the granitoid rocks, as they are most likely to be associated with high fluorine concentrations and, indeed, rare-element mineralization.

A genetic link between fluorine and rare-element mineralization has been demonstrated in several studies (Bailey, 1977; Dingwell *et al.*, 1985; Williams-Jones *et al.*, 2012 and references within). The association of fluorine with rare-element mineralization, in Labrador lake waters, has been recently documented by Amor (2011a, b). However, the relationship between fluorine in till samples and rare-element mineralization has not been investigated in the past.

GEOLOGICAL SETTING

Rock Types

The field area is part of the Meelpaeg Subzone of the Gander Zone, a lithotectonic domain that is in fault-bounded contact with rocks of the Exploits Subzone of the Dunnage Zone to the northwest and southeast (Figure 1; Colman-Sadd, 1986, 1987a, b, 1988). The Exploits Subzone rocks to the northwest are composed of siliciclastic marine sedimentary rocks and mafic volcanic rocks of the Ordovician Red Cross Group, the Silurian Rogerson Conglomerate and felsic and mafic volcanic rocks of the Ordovician Victoria Lake Supergroup (Colman-Sadd, 1986; Valverde-Vaquero *et al.*, 2006). To the southeast the subzone consists of the dominantly volcanic rocks of the Cold Spring Pond Formation and the Pipestone Pond Ophiolite Complex (Colman-Sadd and Swinden, 1982; Swinden and Collins, 1982; Colman-Sadd, 1985; Swinden, 1988; Jenner and Swinden, 1993).

The Meelpaeg Subzone is composed of metasedimentary rocks of the Spruce Brook Formation, intruded by granitic rocks of various ages (Figure 1; Colman-Sadd, 1986, 1987a, b, 1988). The unit is composed of interbedded quartzite, psammite, semipelite and pelite (Plate 1A; Colman-Sadd, 1986). It was subjected to two deformational events and was metamorphosed from greenschist up to sillimanite grade with areas of *in situ* melting that resulted in migmatites and granitoid bodies containing metasedimentary xenoliths. Peak metamorphism postdated the first deformational event and predated the second deformational event (Colman-Sadd, 1986).

The Snowshoe Pond Granite (SPG) is a pink to grey, equigranular, medium-grained, biotite syenogranite (Plate 1B). It also shows evidence for two deformational events (Colman-Sadd, 1986). Valverde-Vaquero *et al.* (2006) dated the SPG at 468 +3.5/-3 Ma (U–Pb zircon), which is similar in age (464 ± 3 Ma U–Pb zircon; Colman-Sadd *et al.*, 1992) to the Great Burnt Lake Granite on the eastern side of the Meelpaeg Subzone and the Peter Strides granite to the southwest (467 ± 6 Ma U–Pb zircon; Valverde-Vaquero *et al.*, *op. cit.*). These granites are geochemically and petrographically similar, and belong to a group of Ordovician peraluminous to metaluminous granites derived from the Gander Group sedimentary rocks by partial melting and mixing with minimum contribution from the mantle; the latter indicated by their negative ε_{Nd} values (Kerr *et al.*, 1995; Kerr, 1997; Valverde-Vaquero *et al.*, 2006).

The North Bay Granite Suite (NBGS) is a composite batholith covering approximately 4000 km² and consisting of 14 phases ranging in composition from granite to granodiorite (Dickson, 1990). Deformation ranges from undeformed to strongly deformed (Dickson, 1990). Strong deformation is localized along the Meelpaeg Lake Fault Zone separating the Wolf Mountain Granite (WMG) and the Meelpaeg Lake Granite (MLG). Three phases are moderately deformed and the rest are undeformed to weakly deformed. Most recent U–Pb zircon dating of the NBGS has yielded 396 +6/-3 Ma for the Dolland Brook Granite (Dunning *et al.*, 1990), 388 ± 4 Ma for the WMG (Kerr and McNicoll, 2012) and 403 ± 3 Ma for the Buck Lake Granite (van Staal *et al.*, 2005). The NBGS is represented by three units in the study area, which include the MLG, pegmatite dykes, and aplite (Figure 1; Colman-Sadd, 1986; Dickson, 1990). The MLG varies from a medium- to coarse-grained, grey to pink, porphyritic biotite granodiorite, to a medium-grained, grey to buff, garnet–muscovite monzogranite. In the current study, trace garnet was identified in only one sample. Local relationships indicate emplacement in the terminal stages of the second deformational event, suggesting a syn- to late-tectonic origin (Colman-Sadd, 1986; Dickson, 1990). Pegmatite dykes cut all other units in the area (Plate 1B). They are composed of a garnet–muscovite ± tourmaline monzogranitic pegmatite and are posttectonic. The mineralogy suggests the pegmatite possibly belongs to the D'Espoir Brook Granite (*see* Dickson, 1990). A fine-grained, garnet–muscovite monzogranitic aplite intrudes the MLG. The WMG occurs south of the current study area and was not sampled, but whole-rock geochemical data of samples collected by W.L. Dickson between 1980 and 1985 were used in this study for comparison (https://geoatlas.
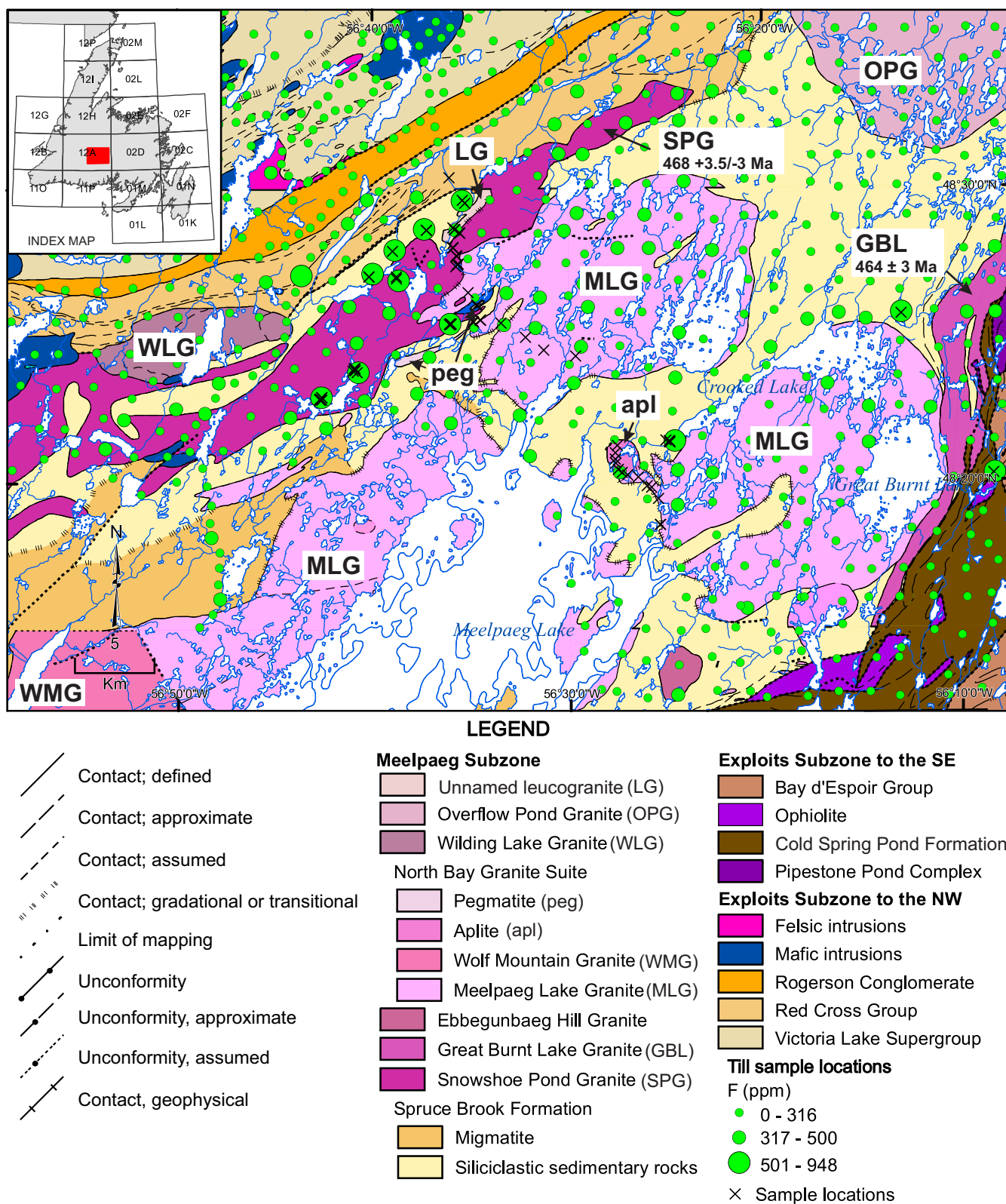
Figure 1. *Geology of the Snowshoe Pond and surrounding areas (modified after Colman-Sadd, 1987b; Swinden, 1988; Colman-Sadd and Swinden, 1984, 1989; Dickson, 1990; Evans* et al.*, 1994a, b). Inset map shows location of study area.*
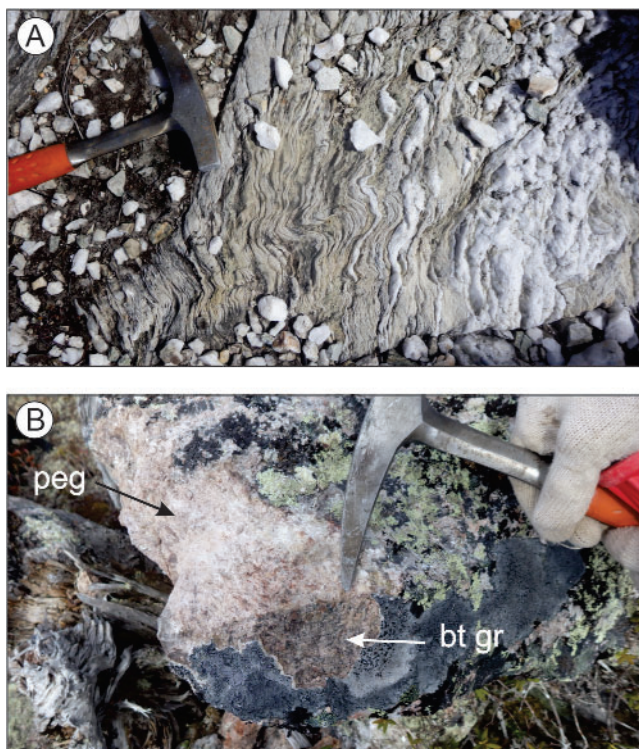
Plate 1. *A) Foliated sedimentary rocks of the Spruce Brook Formation; B) Contact of biotite granite (bt gr) of the SPG and a pegmatite dyke (peg).*

gov.nl.ca). The WMG is a pink to buff, medium- to coarse-grained, K-feldspar porphyritic, muscovite–biotite granite and it is the host of several Mo, W, Pb and fluorite occurrences (Dickson, 1990).

An unnamed leucogranite (LG) occurs north of the SPG and consists of white, medium grained, equigranular granite with quartz, feldspar, minor biotite, chlorite and muscovite and is cut by quartz ± tourmaline veins (Figure 1; Colman-Sadd, 1986, 1987a). It occurs as sills intruding along cleavage planes in foliated SPG (Colman-Sadd, 1986, 1987a). The leucogranite postdates the first deformational event, but may have been deformed by the second deformational event. Sampling of this unit was unsuccessful probably due to the scarce exposure in a densely wooded area. All collected samples in the area were similar in mineralogy and lithogeochemistry to the SPG, suggesting that they were not part of the leucogranite.

Tectonic Evolution of the Meelpaeg Subzone

The Meelpaeg Subzone is interpreted as a metamorphic nappe of Gander Zone metasedimentary rocks (Colman-Sadd and Swinden, 1984; Colman-Sadd *et al.*, 1992; van der Velden *et al.*, 2004) that was emplaced northward over rocks of the Exploits Subzone during the earliest Devonian (Dunning *et al.*, 1990).

Prior to emplacement, during the Middle Ordovician Penobscot Orogeny, ophiolitic rocks of the Dunnage Zone were obducted onto the Gander Zone sedimentary rocks from the west. This resulted in the burial of the Ganderian rocks to a depth sufficient for *in-situ* anatexis of the sedimentary rocks (Colman and Swinden, 1984; Valverde-Vaquero *et al.*, 2006). The SPG, Peter Stride and Great Burnt Lake granites manifest the result of this crustal thickening and anatexis.

The Meelpaeg Subzone was emplaced above the Red Cross Group of the Exploits Subzone along the southeast-dipping Victoria River Thrust, (locally known as Noel Paul's Line), during the Early Devonian Acadian Orogeny (Williams *et al.*, 1988; Valverde-Vaquero and van Staal, 2001; van der Velden *et al.*, 2004). The southeastern boundary of the Meelpaeg allochton is the east-dipping Great Burnt Lake Fault. The Meelpaeg allochthon is interpreted to have formed as an escape structure between the Great Burnt Lake Fault and the Victoria River Thrust. It likely originated from beneath the Bay d'Est–Cinq Cerf thrust sheet to the southeast (van der Velden *et al.*, 2004).

The NBGS is one of the magmatic suites that intruded episodically between late-syn-Salinic and pre-Acadian tectonic events as described by van Staal *et al.* (2014). The reason for this is that in the Early Silurian, Ganderia's leading edge formed the lower plate during the Salinic orogeny, whereas it formed the upper plate along its trailing edge during the Acadian event. Magmatism in the leading edge of Ganderia was caused by slab break-off that resulted in the formation of an asthenospheric window. In the trailing edge of Ganderia, underthrusting of the progressively flattening leading edge of Avalonia and fluid released from the Avalonian slab caused melting and generation of mafic melts in the mantle wedge trapped between Avalonia and Ganderia, which, in turn, melted the overlying crustal rocks to generate felsic magmatism (van Staal *et al.*, 2014).

ANALYTICAL METHODS

Twelve samples of SPG, and pegmatites with anomalously high fluorine contents were selected for qualitative analysis and mineral imaging using a FEI MLA 650FEG(2) Scanning Electron Microscope (SEM) at Memorial University of Newfoundland (MUN) Micro Analysis Facility (MUN MAF-IIC). Qualitative analyses were completed with high throughput Energy-dispersive X-ray spectroscopy (EDX) detectors from Bruker (https://www.mun.ca/creait/). The purpose of the SEM work was to

identify any unknown minerals present, as well as all the elements in the selected minerals for subsequent quantitative analysis with an Electron Probe Microanalyzer (EPMA).

Three of the samples were selected for quantitative mineral chemical analysis at Memorial University of Newfoundland (MUN) using a JEOL JXA-8230 EPMA. The electron microprobe is equipped with 5 wavelength dispersive spectrometers (WDS), a Thermo energy dispersive spectrometer (EDS), an xCLent IV cathodoluminescense (CL) spectrometer, W electron gun and a reflected light optical microscope (https://www.mun.ca/creait/). Operating conditions were 15 kV, 20 nÅ and slightly defocused beam (3 μm). Samples were carbon coated to 200 Å, monitored using brass metal. The purpose of the microprobe analysis is to identify the fluorine-bearing phases and measure their fluorine contents. The analyzed minerals included apatite, fluorite, biotite, muscovite, epidote, allanite, monazite and xenotime. Standards of the same, or similar, minerals with similar composition were inserted at regular intervals. The EPMA is not capable of analyzing lithium because the element is too light. Cesium could not be analyzed due lack of an appropriate standard.

PETROGRAPHY AND MINERAL CHEMISTRY

SNOWSHOW POND GRANITE (SPG)

The SPG is a pink, biotite ± muscovite granite. It is fine to coarse grained, typically equigranular with rare myrmekitic and granophyric textures. The main minerals include quartz, K-feldspar, plagioclase, biotite, muscovite and chlorite (Table 1; Plate 2A–D). The accessory minerals are hematite, epidote, zircon, apatite (Plate 2E), calcite, titanite, fluorite (Plate 2F), monazite, xenotime, thorite, magnetite, ilmenite, rutile, pyrite, chalcopyrite and coltan.

The K-feldspar is microperthitic microcline (Plate 2A, B). Muscovite typically occurs with biotite, or as fine-

Table 1. Average modal mineralogy of the granitoids in the Snowshoe Pond area visually estimated from petrographic analysis

Granite name	Q	Kfp	Pl	Bt	Ms	Gnt	Chl
SPG	39	34	12	5	4		2
MLG	31	21	23	11	5		2
Pegmatite	30	24	27	1	12	3	
Aplite	40	25	22		7	4	
White granite	37	33	17	3	6		4

grained alteration in K-feldspar and in the core of zoned plagioclase (Plate 2C, D). Zircon is common; typically occurring in biotite exhibiting pleochroic haloes. Apatite occurs in micas and/or along grain boundaries of feldspar and quartz (Plate 2E). Rutile occurs as needles in chlorite. Most opaque minerals are typically associated with biotite.

The SPG is weakly to strongly foliated and locally, moderately to strongly, altered. Alteration varies, and includes sericitization of K-feldspar, plagioclase altering to saussurite and possibly K-feldspar (Plate 2B), chlorite ± epidote alteration of biotite, and magnetite altering to hematite. One sample shows evidence of silicification where quartz surrounds and engulfs other minerals; another sample is cut by quartz and chlorite veinlets.

NORTH BAY GRANITE SUITE

Meelpaeg Lake Granite (MLG)

The MLG is a white to pink, biotite ± muscovite, granite to granodiorite. It is fine to coarse grained, and typically equigranular, but locally K-feldspar megacrystic. Myrmekitic texture is common (Plate 3A). Although typically undeformed, it locally displays moderate flattening as shown by preferentially aligned micas. The main minerals include quartz, K-feldspar, plagioclase, biotite, muscovite and chlorite (Table 1). The K-feldspar is all microcline with no perthitic lamellae. Accessory minerals are garnet, apatite, zircon, magnetite, hematite, chlorite, epidote and calcite. Local alteration ranges from weak to moderate with biotite altered to chlorite ± epidote, plagioclase altered to saussurite (Plate 3B, C), and magnetite altered to hematite.

Pegmatite

The pegmatite is very coarse grained (>10 cm), but also contains fine- to medium-grained patches (Plate 4A, B). It contains graphic intergrowth of K-feldspar and quartz, visible in hand sample. The pegmatite consists of quartz, K-feldspar, plagioclase, muscovite, garnet, biotite, apatite (up to 5%) and trace amounts of zircon, monazite, xenotime, magnetite, hematite, pyrite, gahnite ($ZnAl_2O_4$), tourmaline and coltan (Table 1, Plate 4A–F and 5A–E). Beryl has been described from these pegmatites by Colman-Sadd (1986, 1987a, b, 1988). K-feldspar is microcline and locally perthitic, and plagioclase is close to albite in composition. Muscovite is light green and forms either elongated laths, or plumose aggregates intergrown with quartz and plagioclase (Plate 4C, D). Garnet is anhedral to subhedral and zoned with a pink core and light pink to colourless rim. Apatite forms euhedral to anhedral grains (Plate 5A, B). The fine- to medium-grained patches consist of quartz + muscovite ± plagioclase (Plate 4A, B).
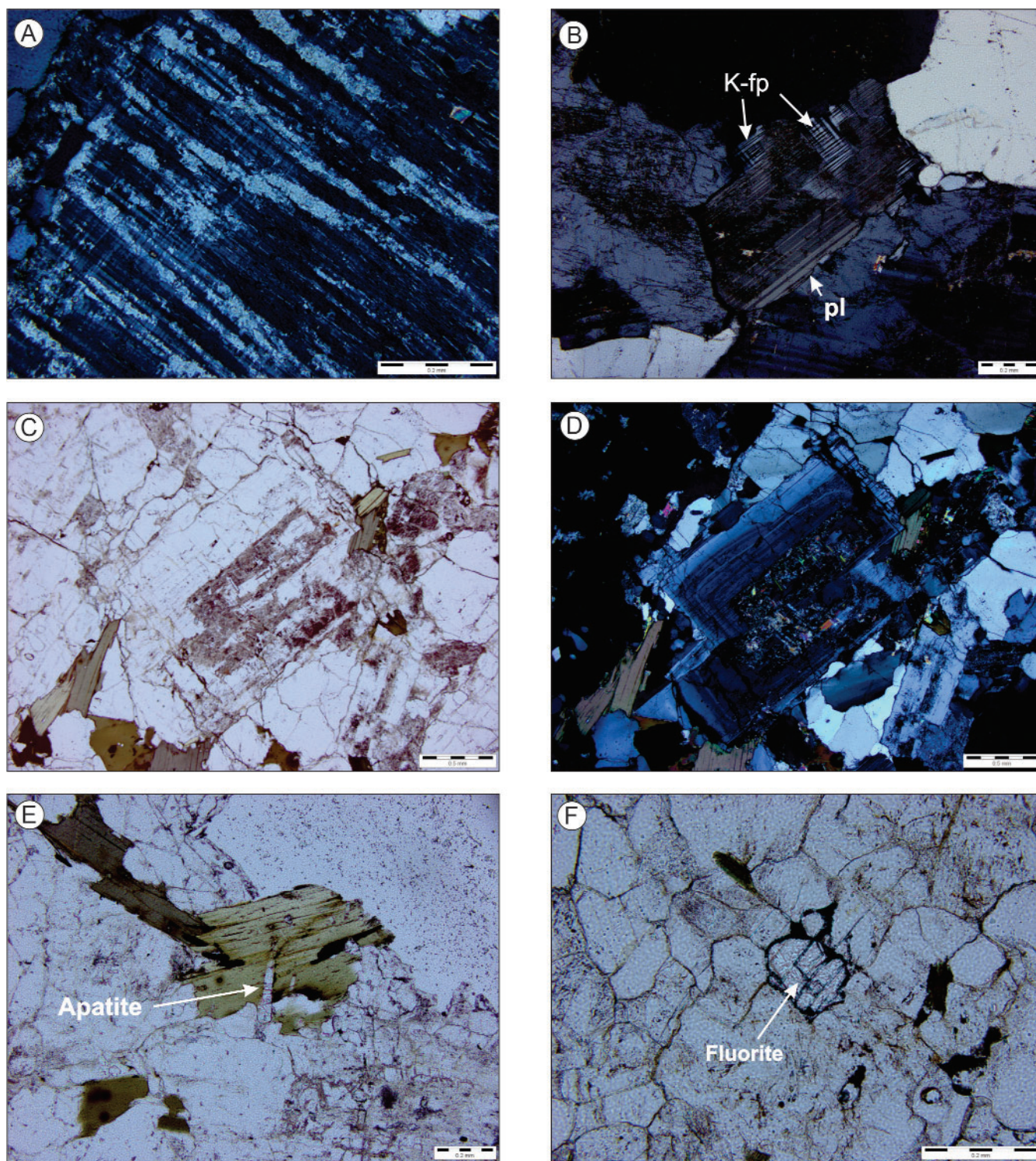
Plate 2. *Photomicrographs of SPG samples. A) Microperthitic microcline; B) Microcline possibly replacing plagioclase; C) Zoned plagioclase saussuratized in the core; D) Same as C under crossed polars; E) Apatite in biotite; F) Fluorite. Key: K-fp–feldspar; pl–plagioclase.*
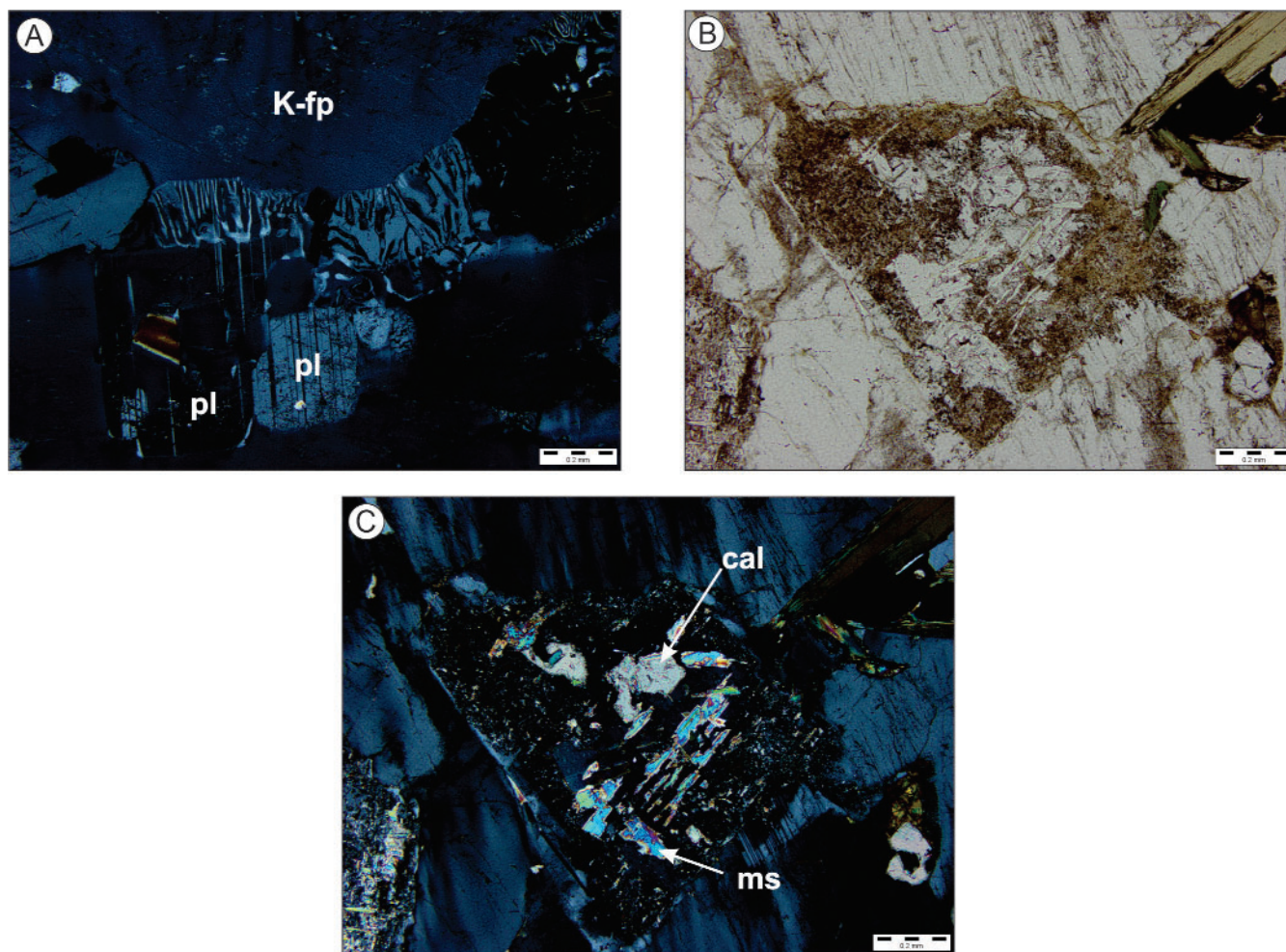
Plate 3. *Photomicrographs of MLG samples. A) Myrmekitic texture at the contact of plagioclase and K-feldspar; B) Plagioclase altered to saussurite (calcite and muscovite) in the core; C) Same as B under crossed polars. Key: K-fp–feldspar; cal–calcite; ms–muscovite; pl–plagioclase.*

The pegmatite is undeformed and locally displays weak to moderate alteration. K-feldspar is albitized in some samples, with albite forming lamellae in and "swapped rows" along grain boundaries of K-feldspar (Plate 4E, F). Both microcline and albite are weakly to moderately altered to sericite or saussurite, respectively. Garnet is locally altered to chlorite, muscovite and/or iron oxides.

Aplite

The aplite is pink, fine to medium grained, with some larger grains of K-feldspar and quartz occurring close to the intrusive contacts with the MLG. It displays very weakly developed myrmekitic texture and is not deformed. It is composed of quartz, K-feldspar, plagioclase, muscovite, garnet and trace amounts of biotite, chlorite, magnetite, hematite, apatite and gahnite (Table 1). K-feldspar is microcline, with no perthitic lamellae, and plagioclase is albite.

Garnet is an- to euhedral and is zoned with a darker core and lighter rim (Plate 5F). The aplite is locally weakly altered, with garnet altered to a fine mixture of chlorite, muscovite and iron oxides, and plagioclase to saussurite.

Mineral Chemistry

The composition of apatite is shown in Table 2 and Figure 2. Apatite in both the SPG and pegmatite is fluorapatite with the fluorine content ranging between 2.06 and 3.12 wt. %. The only significant distinction in the composition of apatite is the Mn content. In the pegmatite, the apatite has between 1.00 and 9.02 wt. % MnO whereas the apatite in the SPG contains less than 0.39 wt. % MnO.

Biotite analyses are presented in Table 3. Biotite in the pegmatite contains 0.89 to 0.97 wt. % F, higher than the fluorine content of biotite in SPG that ranges between 0 and
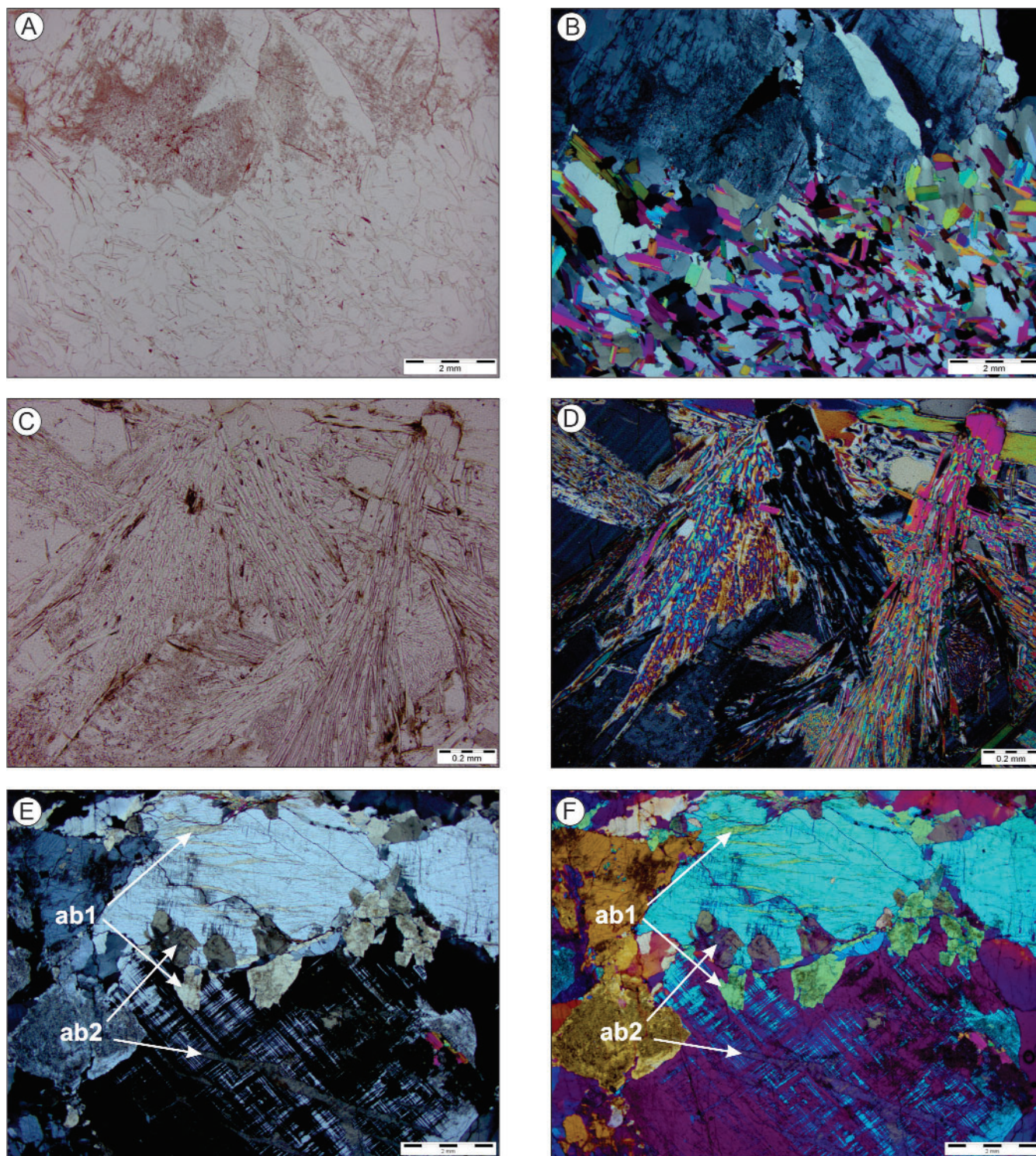
Plate 4. *Photomicrographs of pegmatites. A) Contact of very coarse-grained and medium-grained areas in pegmatite. Very coarse-grained area is composed of K-feldspar and quartz and medium-grained area is composed of muscovite and quartz; B) Same as A under crossed polars; C) Plumose muscovite; D) Same as C under crossed polars; E) Swapped rows of albite along boundary between two K-feldspar grains under crossed polars; F) Same as E using a quartz lense. Key: ab–albite.*

Plate 5. . *A) Subhedral apatite in pegmatite; B) Anhedral apatite along grain boundaries of quartz and feldspars in pegmatite; C) Tourmaline in pegmatite; D) Same as C under crossed polars; E) Back-scattered elect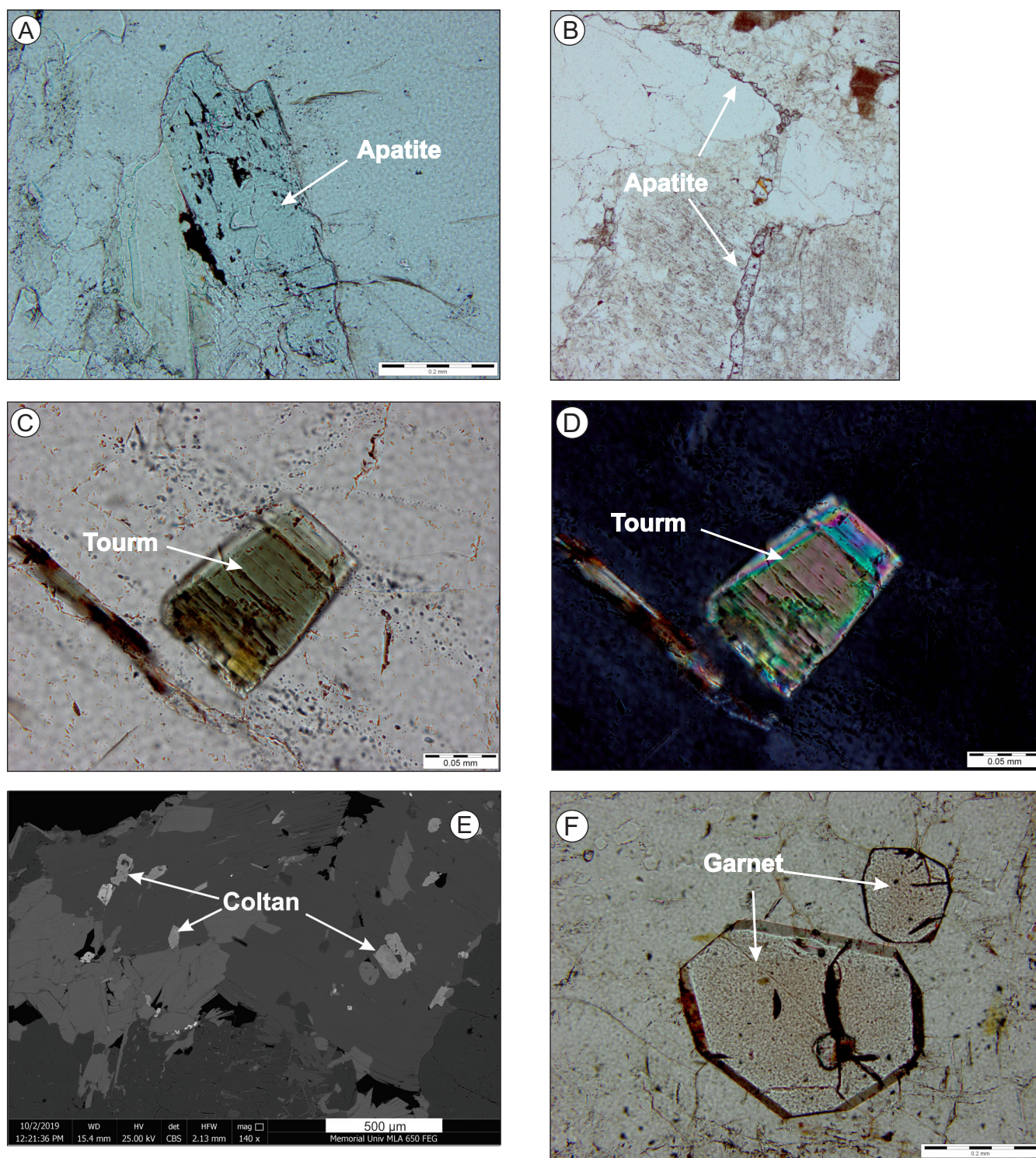ron image of coltan in pegmatite; F) Zoned garnet in aplite. Key: Tourm–tourmaline. Author correction to Plate 5E: Replaced BSE image and caption, May, 2024.*

Table 2. Chemical composition of apatite in wt. % and formula units

	1	2	3	4	5	6	7	8	9	10	11	12	13	14	15
Rock Type	peg	peg	peg	peg	peg	SPG	SPG	SPG	peg	peg	peg	peg	peg	peg	peg
MnO	5.45	2.42	2.74	1.96	6.30	0.18	0.20	0.39	1.00	1.34	1.68	1.18	9.02	4.98	1.00
Nd2O3		0.04	0.05	0.10		0.05	0.11	0.13	0.12		0.07			0.01	
Ce2O3	0.04		0.02	0.04	0.05	0.01	0.05	0.07	0.09	0.13	0.13	0.16	0.01	0.05	0.08
CaO	49.99	53.59	53.03	53.63	48.61	54.86	54.76	54.31	53.63	52.90	52.54	53.37	46.45	50.29	53.90
La2O3	0.01		0.00		0.02		0.01		0.02	0.04	0.07	0.03	0.00		
P2O5	41.76	43.20	42.84	42.90	42.23	42.82	42.89	42.97	42.19	42.29	42.40	42.92	41.86	42.39	42.48
Al2O3	0.00	0.01			0.01	0.00	0.01		0.01		0.00		0.03		0.01
MgO			0.00				0.00	0.01		0.01	0.00	0.01	0.03		
ThO2						0.00		0.02							0.01
Y2O3	0.01		0.04	0.01	0.06	0.21	0.19	0.28	0.35	0.39	0.43	0.40		0.03	0.22
F	2.70	2.65	2.44	2.40	2.79	3.12	2.86	2.57	2.82	2.94	2.76	2.84	2.06	2.47	2.84
Cl	0.02		0.01	0.02	0.01	0.05	0.03	0.04	0.00	0.03			0.03	0.00	
Total	98.59	100.58	99.94	99.84	98.67	99.89	99.78	99.53	98.85	98.62	98.73	99.50	98.40	98.95	99.12

Number of ions on basis of 25 O: A10 X6 O24 (F, Cl, OH)2

|	1	2	3	4	5	6	7	8	9	10	11	12	13	14	15
P	6.028	6.236	6.185	6.193	6.097	6.182	6.191	6.203	6.090	6.105	6.121	6.196	6.043	6.120	6.133
Ca	9.132	9.791	9.688	9.799	8.880	10.023	10.004	9.923	9.797	9.664	9.599	9.751	8.487	9.187	9.847
Mg			0.001				0.001	0.002		0.003	0.001	0.003	0.007		
Mn	0.787	0.349	0.396	0.283	0.910	0.025	0.029	0.056	0.145	0.193	0.243	0.170	1.302	0.719	0.144
La	0.001				0.001		0.001		0.001	0.003	0.004	0.002			
Ce	0.003		0.001	0.002	0.003		0.003	0.004	0.005	0.008	0.008	0.010		0.003	0.005
Nd		0.003	0.003	0.006		0.003	0.007	0.008	0.007		0.004			0.001	
Al	0.001	0.001			0.001		0.003		0.003		0.001		0.006		0.002
Th								0.001							
Y	0.001		0.003	0.001	0.005	0.019	0.018	0.026	0.032	0.036	0.039	0.037		0.003	0.020
Sum A site	9.925	10.144	10.093	10.092	9.801	10.070	10.066	10.020	9.990	9.907	9.900	9.973	9.802	9.913	10.017
F	1.457	1.390	1.289	1.266	1.502	1.646	1.508	1.354	1.505	1.575	1.477	1.502	1.113	1.320	1.512
Cl	0.005		0.002	0.005	0.003	0.013	0.009	0.010	0.001	0.009			0.008	0.001	
OH	0.538	0.610	0.709	0.729	0.495	0.341	0.483	0.635	0.493	0.416	0.523	0.498	0.879	0.679	0.488
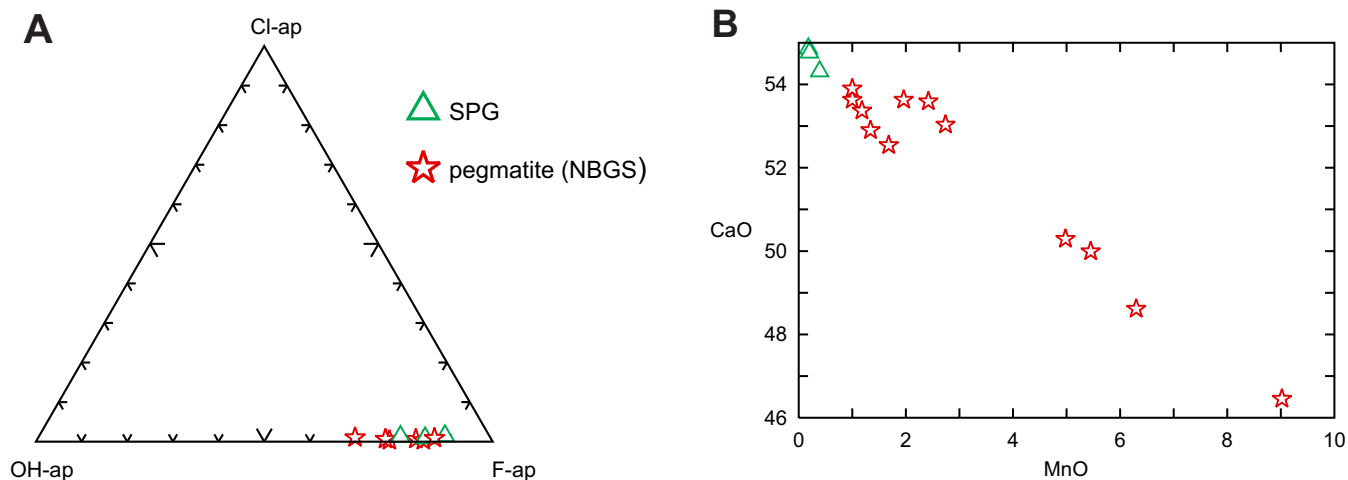
Figure 2. *The composition of apatite. A) Halogen content per formula unit; B) MnO* vs. *CaO contents in wt. %.*

Table 3. Chemical composition of biotite in wt. % and formula units

Rock Type	1 SPG	2 SPG	3 peg	4 peg	5 SPG	6 SPG	7 SPG	8 SPG	9 SPG	10 SPG	11 SPG	12 SPG
SiO2	34.43	34.70	35.21	35.51	33.42	33.60	33.25	34.37	36.63	36.64	36.31	36.13
TiO2	3.07	2.44	2.05	2.56	3.12	2.95	2.38	3.83	2.16	2.23	2.24	2.41
Al2O3	17.44	16.42	15.97	16.42	15.46	14.63	15.97	15.58	17.22	17.00	16.82	16.75
FeO	25.21	23.92	22.48	22.32	33.33	34.22	34.79	31.05	15.85	16.11	17.68	17.60
MnO	0.57	0.18	1.02	1.04	0.55	0.70	0.34	0.72	0.22	0.26	0.23	0.22
MgO	5.05	7.78	7.13	7.25	0.49	0.36	0.31	0.53	12.71	12.40	11.68	11.36
CaO	0.03	0.02	0.00		0.00		0.02	0.02		0.00	0.00	0.00
Na2O	0.06	0.11	0.09	0.08	0.15	0.11	0.13	0.17	0.06	0.11	0.14	0.07
K2O	11.09	11.12	10.65	11.15	10.51	10.73	10.63	10.52	11.69	11.43	11.69	11.69
F		0.44	0.97	0.89					0.70	0.69	0.49	0.65
Cl	0.04	0.03	0.00	0.01	0.06	0.06	0.06	0.07	0.01	0.01	0.02	0.02
P2O5				0.01			0.01	0.01	0.02	0.01		0.03
ThO2			0.02	0.02								
Nb2O5				0.00					0.01			
Y2O3			0.01					0.00			0.01	0.02
Total wt. %	96.76	96.92	95.16	96.87	96.90	97.21	97.65	96.73	96.95	96.54	97.08	96.64

Number of ions on basis of 11 O: A M3 T4 O10 (F, Cl, OH)2

	1	2	3	4	5	6	7	8	9	10	11	12
Si	2.694	2.706	2.788	2.762	2.727	2.754	2.708	2.774	2.744	2.755	2.741	2.743
Al	1.306	1.294	1.212	1.238	1.273	1.246	1.292	1.226	1.256	1.245	1.259	1.257
Sum T site	**4.000**	**4.000**	**4.000**	**4.000**	**4.000**	**4.000**	**4.000**	**4.000**	**4.000**	**4.000**	**4.000**	**4.000**
Ti	0.181	0.143	0.122	0.150	0.192	0.182	0.146	0.233	0.122	0.126	0.127	0.138
Al_M_site	0.303	0.214	0.279	0.267	0.215	0.167	0.241	0.256	0.264	0.262	0.238	0.242
Fe+2	1.650	1.560	1.489	1.452	2.275	2.346	2.369	2.095	0.993	1.013	1.116	1.118
Mn	0.038	0.012	0.068	0.069	0.038	0.048	0.023	0.049	0.014	0.016	0.015	0.014
Mg	0.589	0.905	0.841	0.840	0.059	0.044	0.037	0.064	1.419	1.390	1.314	1.286
Sum M site	**2.761**	**2.834**	**2.800**	**2.777**	**2.778**	**2.788**	**2.816**	**2.696**	**2.812**	**2.808**	**2.810**	**2.798**
Ca	0.002	0.002	0.000	0.000	0.000	0.000	0.001	0.002	0.000	0.000	0.000	0.000
Na	0.009	0.016	0.013	0.012	0.024	0.017	0.020	0.026	0.009	0.016	0.021	0.010
K	1.107	1.106	1.076	1.106	1.094	1.122	1.104	1.083	1.117	1.097	1.126	1.133
Sum A site	**1.118**	**1.124**	**1.089**	**1.118**	**1.119**	**1.139**	**1.126**	**1.111**	**1.126**	**1.113**	**1.147**	**1.143**
F	0.000	0.102	0.225	0.205	0.000	0.000	0.000	0.000	0.161	0.159	0.114	0.150
Cl	0.005	0.004	0.001	0.001	0.008	0.007	0.007	0.009	0.002	0.001	0.003	0.002
OH	1.995	1.895	1.775	1.793	1.992	1.993	1.993	1.991	1.837	1.840	1.883	1.848

0.70 wt. %. Biotite also shows a large range of FeO and MgO contents. The MnO content of biotite in the pegmatite is slightly elevated compared to that of the biotite in the SPG.

Muscovite contains between 0.38 and 0.39 wt. % F in pegmatite and between 0 and 0.63 wt. % F in the SPG (Table 4). The FeO content of muscovite is elevated in both the SPG and the pegmatite, with a range between 2.48 and 4.10 wt. %. The Ti and Mg contents are also elevated. Fluorite was identified in one SPG sample. The fluorine content of the fluorite is 48.13 wt. %. One allanite grain in the SPG, an epidote series mineral, returned 0.14 wt. % F. Monazite from the SPG contains between 0.26 and 0.46 wt. % F.

GEOCHEMISTRY

Most of the granitoid rocks plot in the granite field, although the MLG ranges from granite to granodiorite

Table 4. Chemical composition of muscovite in wt. % and formula units

Rock Type	1 SPG	2 peg	3 peg	4 SPG	5 SPG	6 SPG	7 SPG
SiO2	48.42	47.18	47.98	46.48	46.83	47.48	47.17
TiO2	1.08	0.85	0.98	1.51	1.05	0.02	0.10
Al2O3	31.98	32.57	32.25	32.52	33.16	36.34	34.45
FeO	4.10	3.74	3.76	3.90	3.71	2.48	3.74
MnO	0.01	0.10	0.09		0.01	0.04	0.09
MgO	1.39	1.40	1.52	1.09	1.00	0.39	0.53
CaO	0.00		0.00			0.01	0.01
Na2O	0.48	0.77	0.63	0.48	0.63	1.07	0.77
K2O	12.23	11.91	11.67	12.09	12.08	11.79	11.93
F	0.27	0.38	0.39			0.49	0.63
Cl	0.00	0.01	0.00	0.00			0.00
P2O5	0.00	0.01	0.01	0.01		0.04	0.03
ThO2		0.00		0.01		0.03	
Nb2O5		0.04	0.01			0.02	0.05
Y2O3						0.02	0.00
Total wt. %	99.79	98.76	99.11	98.05	98.37	100.00	99.23

Number of ions on basis of 11 O: A M3 T4 O10 (F, Cl, OH)2

Si	3.156	3.110	3.141	3.084	3.089	3.063	3.093
Al	0.844	0.890	0.859	0.916	0.911	0.937	0.907
Sum T site	4.000	4.000	4.000	4.000	4.000	4.000	4.000
Al	1.612	1.641	1.630	1.627	1.666	1.827	1.755
Ti	0.053	0.042	0.048	0.075	0.052	0.001	0.005
Fe+2	0.224	0.206	0.206	0.217	0.205	0.134	0.205
Mn	0.001	0.006	0.005		0.001	0.002	0.005
Mg	0.135	0.138	0.148	0.108	0.098	0.038	0.052
Sum M site	2.024	2.032	2.038	2.027	2.022	2.001	2.022
Ca	0.000		0.000			0.000	0.000
Na	0.061	0.099	0.080	0.062	0.080	0.134	0.098
K	1.017	1.002	0.975	1.024	1.017	0.970	0.998
Sum A site	1.078	1.101	1.055	1.085	1.097	1.105	1.097
F		0.063	0.087	0.090			0.112	0.146
Cl	0.000	0.002	0.000	0.000			0.000
OH	1.936	1.912	1.909	2.000	2.000	1.888	1.853

(Figure 3A). A few pegmatite samples fall in the alkali granite field. The granitoids are dominantly peraluminous, having alumina saturation indices (ASI = Al/(Ca - 1.67P + Na + K); (Frost and Frost, 2008 and references within) greater than 1.1, with the exception of those of the SPG that are mostly metaluminous (Figure 3B). All samples straddle the boundary between A-type and I- and S-type granites (Figure 3C; Whalen *et al.*, 1987).

All granites show a negative correlation between SiO$_2$ and Al$_2$O$_3$ (Figure 4A). K$_2$O shows a weak positive correlation with SiO$_2$ in the MLG and a negative correlation in the other granites, whereas SiO$_2$ shows a weak negative correlation with Na$_2$O in the MLG and a positive correlation in the other granites (Figure 4B, C). CaO shows a negative corre-
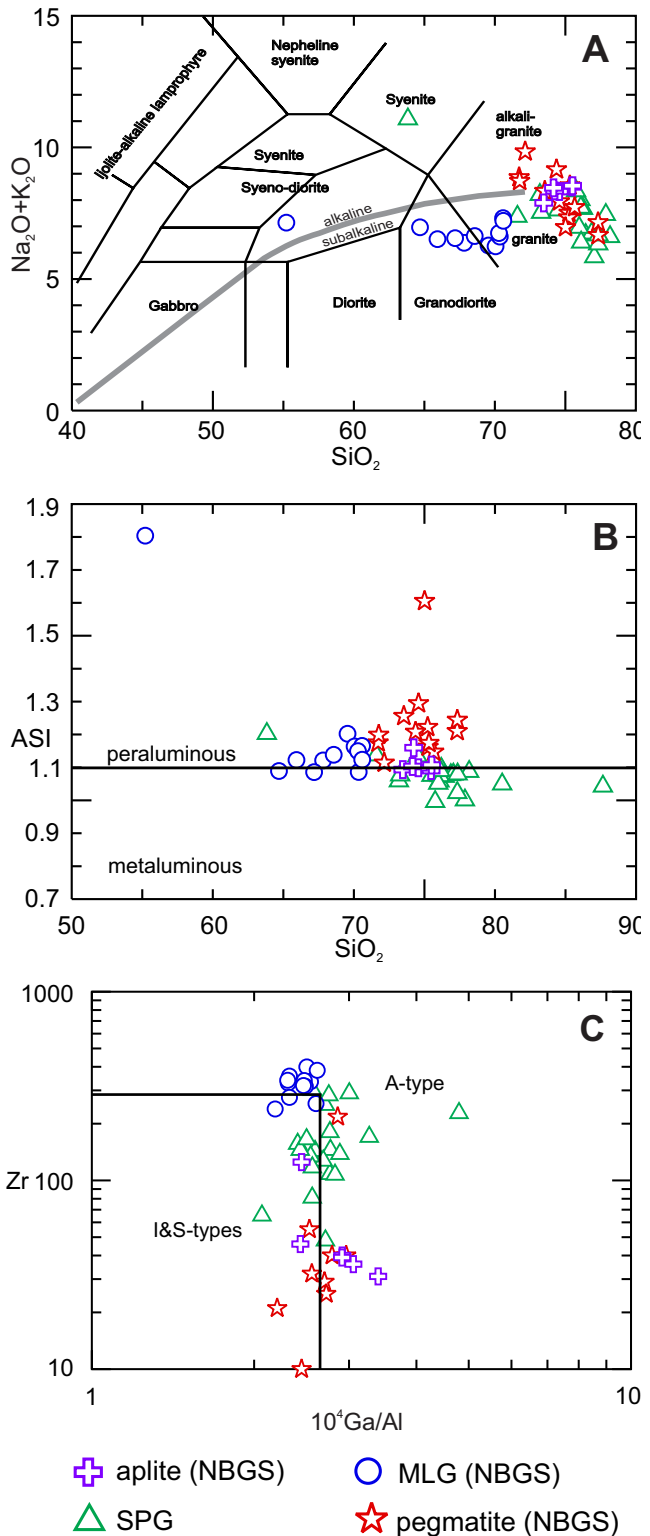

Figure 3. *A) Rock types (after Cox* et al., *1979; Wilson, 1989); B) Aluminum saturation index (ASI = Al/(Ca - 1.67P + Na + K) of the granitoids (after Shand, 1922); C) Type of granitoids (Whalen* et al., *1987).*
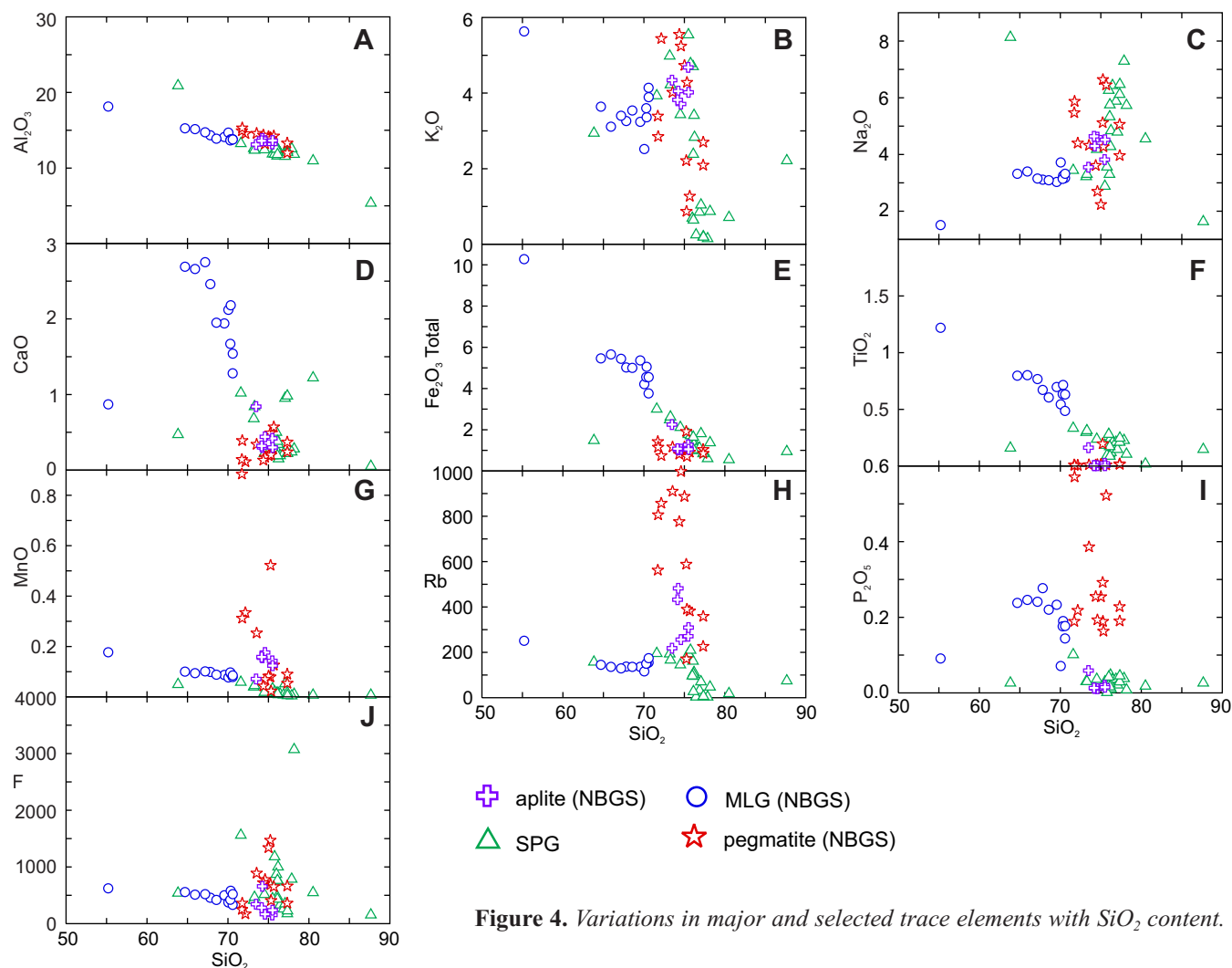
Figure 4. *Variations in major and selected trace elements with SiO₂ content.*

lation with SiO₂ in the MLG (Figure 4D). The total iron, TiO₂ and MnO show a negative correlation with SiO₂ in all units (Figure 4E, F). MnO displays two distinct trends (Figure 4G), a steeper trend defined by the pegmatite and aplite and a more gradual trend by the MLG and SPG. In addition to MnO, the pegmatite also displays higher concentrations of Rb and P₂O₅ compared to the other units (Figure 4H, I). The fluorine content is highest in the SPG and pegmatite, and shows a negative correlation with SiO₂ in the MLG (Figure 4J). Samples of the Spruce Brook Formation metasedimentary rocks were not plotted, but they locally contain elevated fluorine values up to 1680 ppm. The pegmatite also displays higher concentrations of Be, Cs, Ta and Li, and lower concentrations of Zr and Th than the other units (Figure 5A–C).

Whereas the chondrite-normalized REE signatures of most of the units are very distinct with variably developed negative Eu anomalies, variable, but ubiquitous, REE

enrichment, and variable LREE enrichment, the pegmatite does not show any significant enrichment in REEs (Figure 6). In the MLG and SPG, the LREEs are more strongly enriched with a negative slope for both the LREEs and HREEs. In the aplite, the REEs have flat patterns, with moderate Eu troughs. The pegmatite and aplite are enriched in Cs, Rb, U, Li and Ta relative to the upper continental crust and the SPG and MLG (Figure 6; Rudnick and Gao, 2003).

Barium and Sr contents suggest plagioclase fractionation in the MLG, and likely both plagioclase and K-feldspar fractionation in the other units (Figure 7A, B; Yu *et al.*, 2007). Based on the Nb/Ta *vs.* Ta plot, the pegmatite is the most fractionated, followed by aplite, SPG, and MLG (Figure 7C; Linnen and Cuney, 2005).

The tectonic setting of the granitoids varies (Figure 8; Pearce *et al.*, 1984). The SPG and the aplite fall mostly in the within-plate granite (WPG) field, the MLG falls mostly
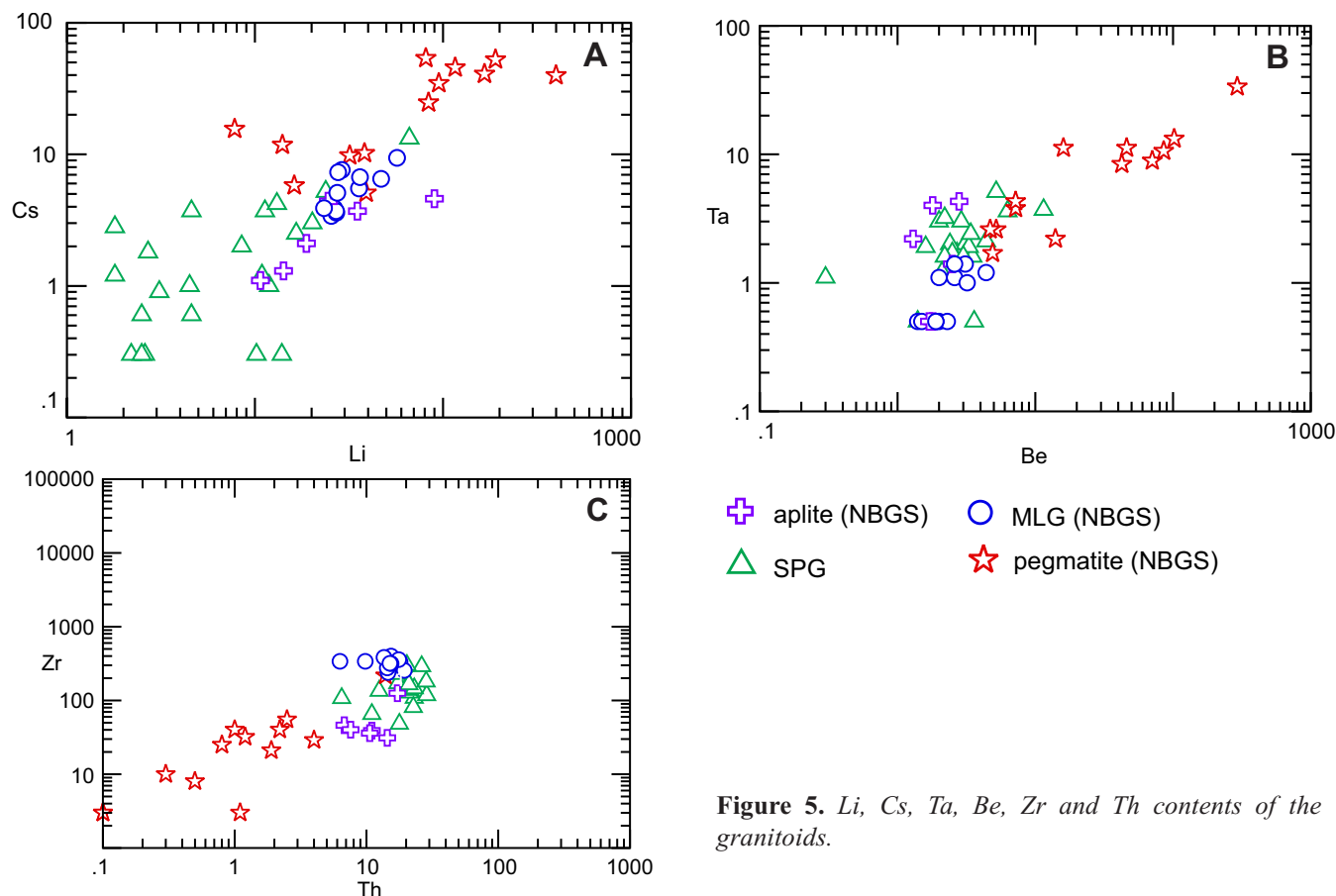
Figure 5. *Li, Cs, Ta, Be, Zr and Th contents of the granitoids.*

in the volcanic arc granite (VAG) field and the pegmatite falls in the syn-collisional granite (syn-COLG) field. Although, the tectonic setting for pegmatite and aplite indicated by these diagrams may be misleading due to volatile fluxing (Pearce *et al.*, 1984).

On the Na$_2$O+K$_2$O *vs.* SiO$_2$ diagram, the MLG plots in the W mineralization field and the rest of the units plot in the Sn mineralization field (Figure 9; Azadbakht *et al.*, 2019 and references within). In a Zr/Hf *vs.* SiO$_2$ diagram, the majority of the pegmatite and aplite samples plot in the Li–F granite field, whereas other samples of the pegmatite and SPG fall in the field of granites associated with Sn–W–Mo–Be greisen-type deposits (Figure 9; Azadbakht *et al.*, 2019 and references within). The MLG samples range from granodiorite to biotite granite.

DISCUSSION

SOURCE OF ELEVATED FLUORINE

In the pegmatites, the main fluorine-bearing minerals include muscovite and apatite. Anomalously high fluorine values are the result of the greater modal percent apatite (up

to 5%) in the pegmatite. In the SPG, the fluorine-bearing phases include biotite, muscovite, fluorite, apatite, allanite and monazite. The source of elevated fluorine values varies, or is uncertain, as not all of the micas contain fluorine and only one sample contains fluorite. The rest of the phases, including apatite, occur in trace amounts.

ECONOMIC POTENTIAL OF GRANITOIDS FOR RARE-ELEMENT MINERALIZATION

The pegmatites in the Snowshoe Pond area are Li–Cs–Ta enriched (LCT), or rare-element-enriched pegmatites, which are well known for their association with economic concentrations of rare elements in the Superior Province in Ontario and Manitoba among other places (Selway *et al.*, 2005 and references within; London, 2016). Pegmatites may also be sources of gem stones (*e.g.*, beryl, topaz) and high-quality feldspar, quartz and mica used for glasses, ceramics, electronics and fillers (London, 2016 and references within). In the Superior Province, LCT pegmatites typically occur along major tectonic boundaries, or in metasedimentary-rock-dominant areas. They are hosted in various rock types, but most commonly occur in metavolcanic and metasedimentary rocks, where the grade of meta-
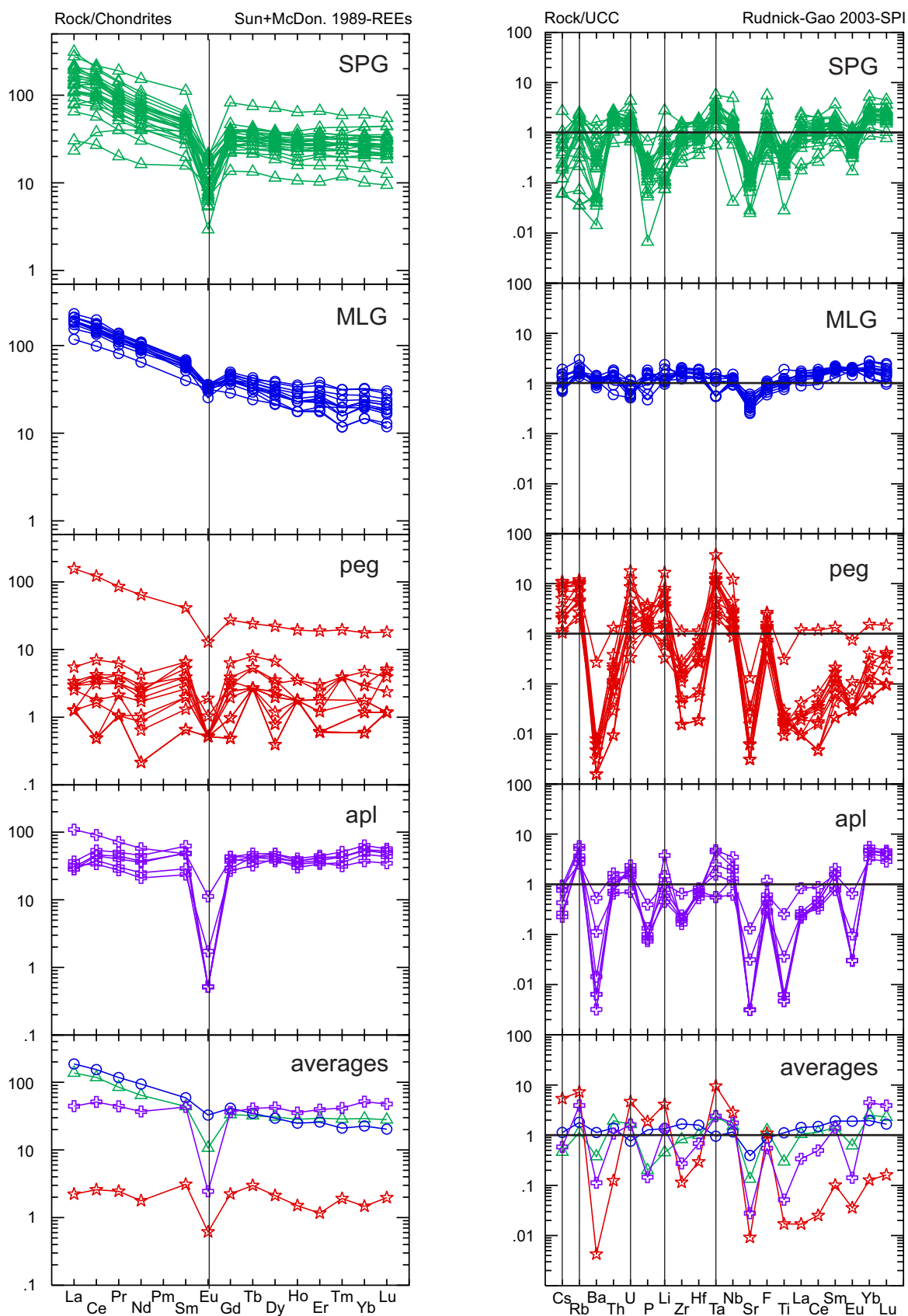
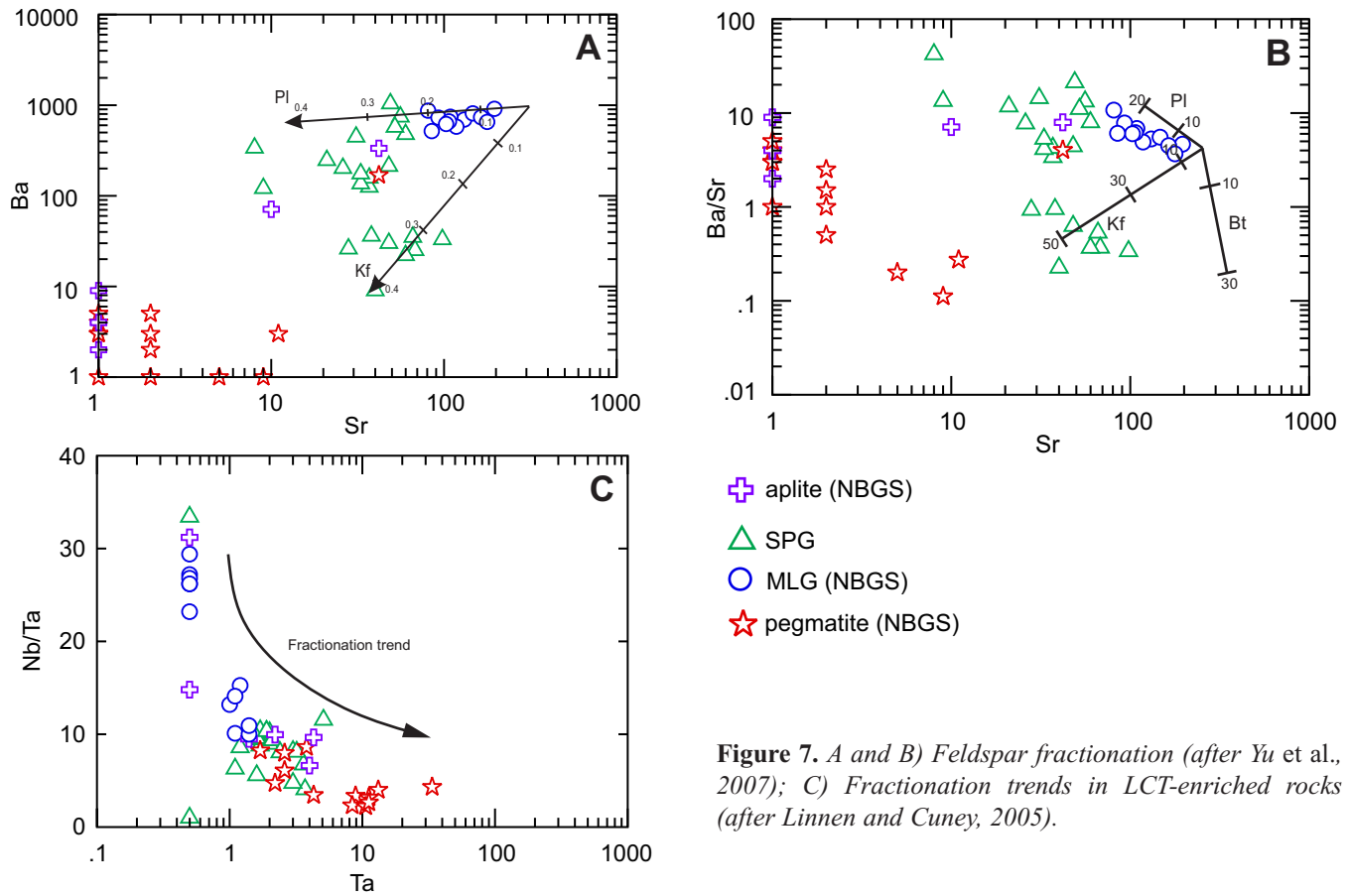**Figure 6.** *Spider diagrams of REE and trace elements (Sun and McDonough, 1989; UCC=upper continental crust).*

Figure 7. *A and B) Feldspar fractionation (after Yu et al., 2007); C) Fractionation trends in LCT-enriched rocks (after Linnen and Cuney, 2005).*
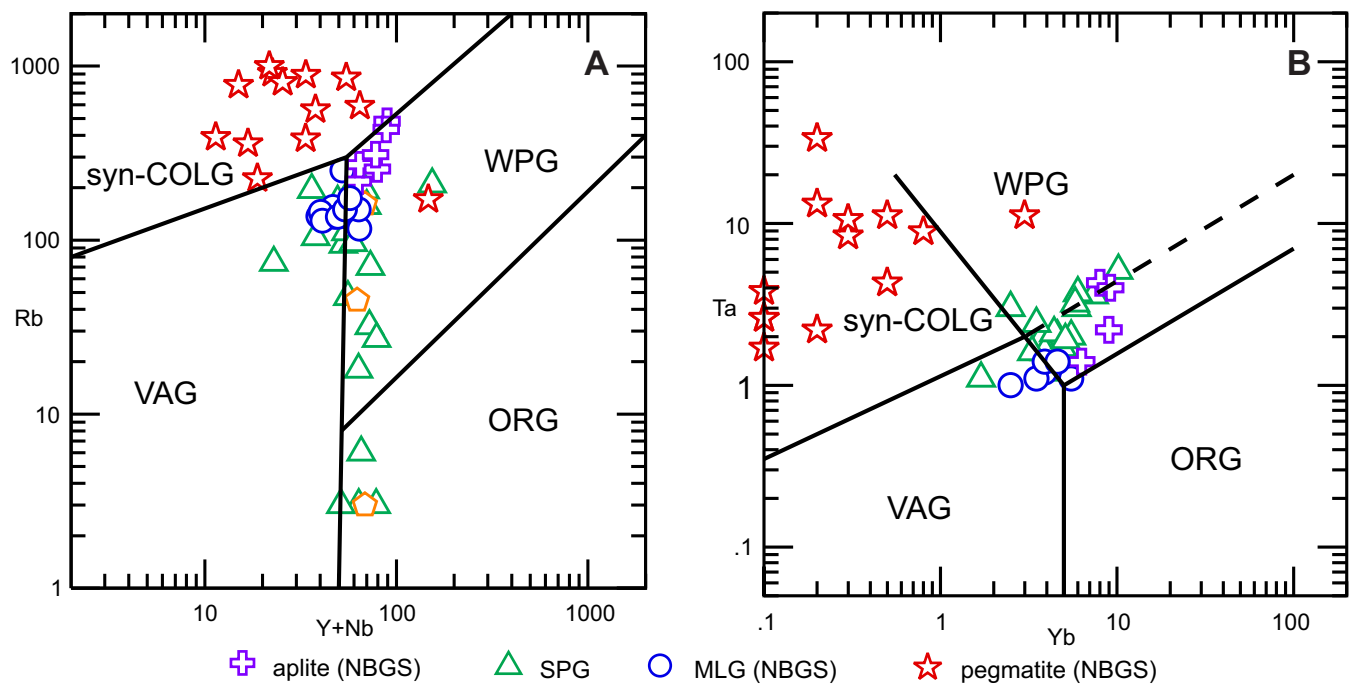

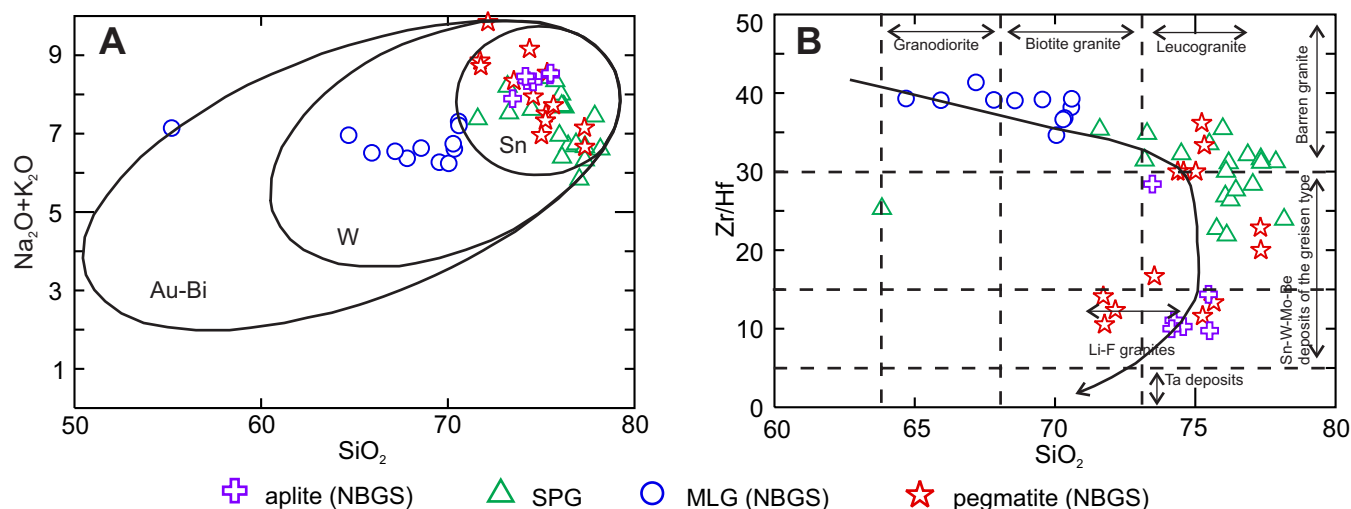**Figure 8.** *Tectonic setting of the granites (after Pearce et al., 1984).*

Figure 9. *Mineralization potential of the granitoids (see Azadbakht et al., 2019 and references within).*

morphism ranges between greenschist and amphibolite facies. The host rocks are metasomatized around the pegmatite and have elevated Li, Rb, Cs, B and F contents, along with the presence of tourmaline, Rb- and Cs-rich biotite, holmquistite, muscovite and garnet.

Most of the rare-element pegmatites, but not all, are genetically derived from a fertile parent granite of the same age (Selway *et al.*, 2005 and references within; London, 2016). The fertile granite is an evolved granite that consists of several phases representing different degrees of fractionation. The residual melt from this granite migrates into the host rocks and crystallizes as pegmatite dykes (Jahns and Burnham, 1969; London, 2016). Fertile granites associated with LCT pegmatite dykes are typically S-type, peraluminous granites (Černý, 1991a, b). The S-type granites are enriched in Li and Cs compared to other granites due to the dehydration melting and decomposition of muscovite in the metasedimentary source rocks; since muscovite is a major reservoir for the incompatible elements Li and Cs along with Rb, Be and Ba (London, 2005, 2016). Fractionation of these granites leads to further enrichment in these incompatible elements. Rare-element pegmatites are typically distributed over a 10 to 20 km^2 area within 10 km of the fertile granite (Breaks and Tindle, 1997). Fertile granites and associated pegmatites show a distinct geochemical, mineralogical and textural zoning internally and with increasing distance from the granite (Figure 10; Jahns and Burnham, 1969; Černý, 1991a, b; Selway *et al.*, 2005; London, 2016). This is caused by increasing fractionation and volatile enrichment, which results in greater enrichment in rare elements and, hence, greater economic potential with increasing distance (up to 10 km) from the parent granite (Selway *et al.*, 2005 and references within; London, 2016). Table 5 shows the rare-element composition of fertile granites compared (Černý,
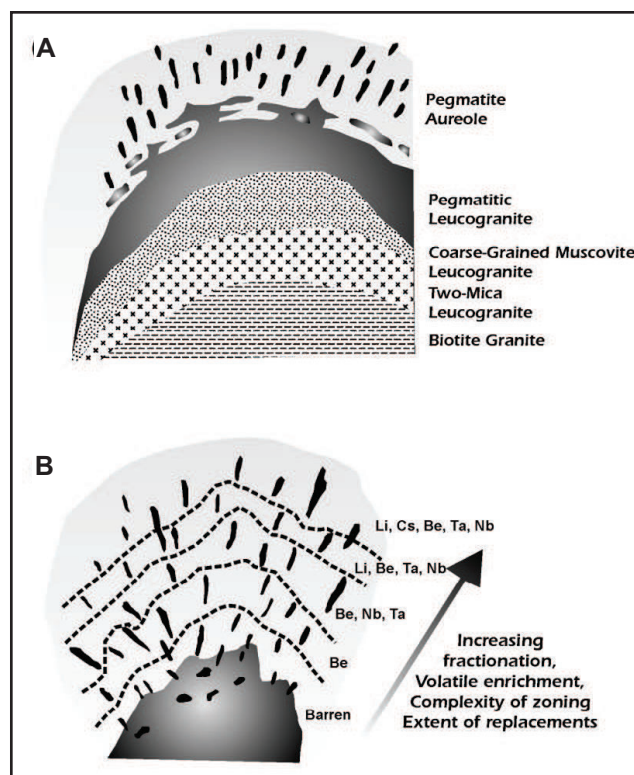

Figure 10. *A) Zoning of a fertile granite with an aurole of Li-pegmatites; B) Zoning in a parent magma and associated pegmatites (modified after Černý, 1991a).*

1989) to the MLG and WMG (https://geoatlas.gov.nl.ca). Table 6 shows the composition of the more fractionated phases of a fertile granite and associated pegmatites in the Superior Province (Černý and Meintzer, 1988) compared to the upper continental crust (Rudnick and Gao, 2003) and pegmatites and aplite from the Snowshoe Pond area.

137

Table 5. Rare-element composition and diagnostic element ratios in fertile granites (Černý, 1989) compared to the MLG and Wolf Mountain Granite (https://geoatlas.gov.nl.ca)

Element/ Ratio	Fertile Granites Range	MLG Mean	Range	Wolf Mountain Mean	Range
Ti	<100–4300	4278	2910–7306	1257	420–3177
Sr	<1–445	126	81–196	103	23–251
Ba	6–900	710	517–912	306	32–573
Zr	<1–77	323	239–399	116	20–210
Li	1–3,540	32	23–57	76	31–162
Be	1–604	2	1–4	6	3–9
Ga	19–90	19	17–25		
Rb	32–5775	151	116–251	270	168–440
Cs	3–51	6	3–9		
Y	3–102	37	26–53	15	4–41
Sn	<1–112	5	3–6		
K/Rb	42–270	199	181–222	154	82–194
K/Cs	1600–15 400	5,788	3983–7978		
K/Ba	48–18 200	43	33–63	194	70–1185
Rb/Sr	1.6–185	12	10–16	4	1–19
Mg/Li	1.7–50	251	130–363	34	7–86
Al/Ga	1180–3100	4,106	3774–4449		
Zr/Hf	14–64	38	35–41		

The geological setting of the Snowshoe Pond pegmatite dykes is similar to that of the Superior Province pegmatites. They are located close to a major structural boundary between the Exploits and Meelpaeg subzones, and several are hosted in metasedimentary rocks of the Spruce Brook Formation. The grade of metamorphism ranges from greenschist to amphibolite facies, but is locally higher. Elevated fluorine concentrations in various minerals, and the presence of minerals such as coltan in the SPG, most likely represent metasomatic alteration around a nearby pegmatite dyke, rather than a more fractionated phase of the SPG. The metasedimentary rocks also locally contain elevated fluorine concentrations.

The rare-element contents and diagnostic element ratios in the pegmatites from the Snowshoe Pond area indicate that they represent the pegmatitic leucogranite phase of a fertile granite, with the exception of the Nb/Ta ratio, which is slightly higher in the Snowshoe Pond pegmatites (Table 6, Figure 10). The mineralogy of the pegmatites is typical of a pegmatitic leucogranite consisting of megacrystic K-feldspar having graphic quartz intergrowths, quartz, muscovite with common plumose texture, and garnet (Plates 4 and 5; Selway *et al.*, 2005). The Li, Cs and Rb contents of the minerals could not be determined, but the light green muscovite suggests that it may be Li-bearing (Selway *et al.*, 2005). Accessory minerals include apatite, zircon, tourmaline and gahnite, and previous workers (Colman-Sadd, 1986, 1987a, b, 1988) have also described beryl. Coltan was identified suggesting the presence of rare-element-rich pockets, another characteristic of rare-element pegmatitic leucogranite (Selway *et al.*, 2005). The presence of finer grained patches composed of quartz + muscovite ± plagioclase within very coarse-grained patches with K-feldspar, is typical of this phase (Plate 4A, B; Selway *et al.*, 2005). Jahns and Burnham (1969) explains this by crystallization from a coexisting aqueous fluid and silicate melt, where coarser grained K-rich patches crystallize from the aqueous fluid and fine-grained Na-rich patches crystallize from the silicate melt. However, according to London (2016 and references within), this is the result of liquidus undercooling, nucleation delay, followed by the growth of crystals from a highly viscous melt in the absence of an aqueous fluid.

The aplite from the Snowshoe Pond area does not seem to correlate well with the sodic aplite composition of the Superior Province. It does not display the degree of fractionation of a typical sodic aplite, and it contains K-feldspar in addition to albite, garnet, and tourmaline. The aplite in the Snowshoe Pond area ranges up to medium grained and is

Table 6. Average composition and ranges of rare elements in Superior Province pegmatite phases compared to the upper crust (Černý and Meintzer, 1988; Rudnick and Gao, 2003) and pegmatite and aplite in the Snowshoe Pond area (last 4 columns)

Element/ Ratio	Average Upper-Continental Crust	Fine-grained Leucogranite Mean	Range	Pegmatitic Leucogranite Mean	Range	Sodic Aplite Mean	Range	Pegmatite Mean	Range	Aplite Mean	Range
Be	2.1	4	<0.5–61	27	<0.5–604	6	1–34	56.9	4.7–292.9	2.0	1.3–2.8
Cs	4.9	8	<0.5–39	14	<0.5–51	16	<0.2–67	26.3	5.1–53.8	2.8	1.1–4.6
Ga	17.5	38	<10–81	20	<10–90	9	45–73	21.3	17.2–33.4	20.4	16.5–24.9
Li	24	81	1–1400	51.7	6–288	82	7–324	98.7	7.8–399.4	32.3	10.7–90.1
Nb	12	24	<1–81	18	<1–135	-	45–138	34.0	10.4–144.8	21.0	7.4–41.5
Rb	84	305	33–1050	473	32–5780	169	9–559	610.2	171.3–997.1	328.1	217.7–481.8
Sn	2.1	9	<1–44	19	<1–112	13	2–25	21.3	9.7–44.1	9.6	4.9–18.0
Ta	0.9	4.5	2–8.5	2.7	0.5–8	-	3–435	8.6	1.7–33.6	2.2	0.5–4.3
K/Cs	4804	11 000	794–78 400	7880	246–38 500	3020	166–14 900	1695	428.9–3,494.3	16 380	7392–31 113
K/Rb	280	159	42–418	165	13–576	85	24–332	51.6	27.8–91.3	113.8	70.1–166.2
Nb/Ta	13.3	5	0.1–11.9	1.71	0.1–7.17	-	0.32–0.62	4.9	2.2–8.7	13.6	6.7–31.2

always in contact with, or entirely enclosed within, the MLG; suggesting that it is a more fractionated part of the MLG.

The presence of a fertile parent granite for the Meelpaeg nappe pegmatites was not confirmed in this study. All the granites in the area contain both K-feldspar and plagioclase suggesting that they are rich in water, therefore capable of producing larger volumes of pegmatites (Jahns and Burnham, 1969). The SPG is significantly older than the NBGS and is not enriched in rare elements. Of the sampled granites, the most obvious parent granite would be the MLG due to its proximity to the pegmatites, and younger age. However, the degree of fractionation observed for the MLG through incompatible elements is not sufficient for it to be a fertile granite (Table 5), as its upper continental crust normalized profile is flat and it is only weakly enriched in Rb and Li (Figure 6). A possible fertile granite would be a granite similar to the WMG, which seems to be one of the most fractionated granites of the NBGS (Table 5). It is also enriched in Li compared to the upper continental crust (UCC) and other granites with values in excess of 100 ppm (Dickson, 1990; https://geoatlas.gov.nl.ca). The WMG is one of the youngest phases of the NBGS, it is only locally deformed and is interpreted to be late- to posttectonic (Dickson, 1990), a feature inherent in fertile granites (Selway *et al.*, 2005). However, the closest documented outcrop of the WMG is more than 10 km from the study area, too far to be the parent granite of the pegmatite dykes. The fertile granite is more likely located below the pegmatite dykes, underneath the SPG and the northernmost lobe of the MLG. The WMG may extend northeastward into this area, or alternatively, another hidden granite intrusion, similar in age and geochemistry, may occur beneath the study area. The unnamed leucogranite, outcropping over a small area as sills intruding along cleavage planes in foliated SPG (Figure 1; Colman-Sadd, 1986, 1987a) may be another candidate for a fertile parent granite. It postdates the first regional deformation event and may have been affected by the second event, suggesting a late- to posttectonic setting of emplacement. Samples of this unit were not collected for reasons mentioned earlier.

The WMG of the NBGS is one of the few intrusions associated with known occurrences of W, Mo, Bi, Zn and F. Therefore, the possible existence of a similar granitic body in the Snowshoe Pond area is also significant for the potential for additional mineralization of similar nature.

INDICATOR POTENTIAL OF FLUORINE IN TILL SAMPLES

In the Snowshoe Pond and surrounding areas, anomalously high fluorine in till samples (up to 948 ppm) is spatially associated with rare-element-enriched pegmatite dykes. However, further research is needed to assess the economic potential of the pegmatites. A compilation of till sample analyses, including fluorine, over areas with known rare-element mineralization is necessary to assess the use of fluorine concentrations in till samples as positive indicators for economic quantities of rare-element mineralization. Fluorite was found in only one sample in the study area. Therefore, the anomalous F in till samples does not indicate the presence of fluorite mineralization in this area.

FURTHER WORK

Further exploration for rare-element mineralization in the area should include detailed sampling of all rock types to identify metasomatic alteration derived from possible unexposed proximal pegmatite dykes (Selway *et al.*, 2005). Metasomatic alteration will be represented by elevated Li, Cs, Rb, H_2O, B, F, Sn and Be contents and the presence of minerals enriched in these elements, including biotite and holmquistite (Li-rich amphibole: $Li_2Mg_3Al_2Si_8O_{22}(OH)_2$).

If successful in identifying additional pegmatites or a fertile parental granite, this strategy should be followed by an examination of large-scale internal zoning in such fertile granite and pegmatite dykes in order to determine fractionation trends. This process may help in locating pegmatites with the highest potential for economic rare-element mineralization as it is known that the degree of fractionation is directly correlated with the economic potential of the pegmatite (Selway *et al.*, 2005). Fractionation trends can be determined with whole-rock compositions and bulk K-feldspar and muscovite compositions. A mineralogical study of the pegmatites and potential fertile parent granite, with emphasis on the composition of K-feldspar and micas (Rb, Cs, Li and Ta contents), garnet (Fe and Mn contents), tourmaline, beryl (Cs content) and coltan (Fe, Mn, Nb, Ta contents), may also help in determining fractionation trends.

ACKNOWLEDGMENTS

REFERENCES

Amor, S.D.
2011a: Lake-sediment and water-sampling survey in the Fraser Lake region, western Labrador. *In* Current Research. Government of Newfoundland and Labrador, Department of Natural Resources, Geological Survey, Report 11-1, pages 1-14.

2011b: An untested rare-earth element target in northern Labrador. Government of Newfoundland and Labrador, Department of Natural Resources, Geological Survey, Open File 014E/0229, 38 pages.

Azadbakht, Z., Rogers, N., Lentz, D.R. and McFarlane, C.R.M.
2019: Petrogenesis and associated mineralization of Acadian related granitoids in New Brunswick. Targeted Geoscience Initiative: *In* 2018 Report of Activities. *Edited by* N. Rogers. Geological Survey of Canada, Open File 8549, pages 243-278.

Bailey, J.C.
1977: Fluorine in granitic rocks and melts: A review. Chemical Geology, Volume 19, pages 1-42.

Breaks, F.W. and Tindle, A.G.
1997: Rare element exploration potential of the Separation Lake area: An emerging target for Bikita-type mineralization in the Superior Province of north-west Ontario. In Summary of Field Work and Other Activities, 1997. Ontario Geological Survey, Miscellaneous Paper 168, pages 72-88.

Campbell, H.
2018: Till-geochemistry survey in the Great Burnt Lake (NTS 12A/08), Burnt Hill (NTS 2D/05), northern Cold Spring Pond (NTS 12A/01) and adjacent map areas. Government of Newfoundland and Labrador, Department of Natural Resources, Geological Survey, Open File NFLD/3341, 10 pages.

2019: Till geochemistry of the Great Burnt Lake (NTS 12A/08), Burnt Hill (NTS 2D/05), northern Cold Spring Pond (NTS 12A/01) and adjacent map areas. Government of Newfoundland and Labrador, Department of Natural Resources, Geological Survey, Open File NFLD/3358, 54 pages.

Campbell, H., Organ, J.S. and Taylor, D.
2017: Till-geochemistry sampling and quaternary mapping in south-central Newfoundland, Great Burnt Lake (NTS 12A/08), northern Cold Spring Pond (NTS 12A/01), and Burnt Hill (NTS 2D/05) map areas. *In* Current Research. Government of Newfoundland and Labrador, Department of Natural Resources, Geological Survey, Report 17-1, pages 105-117.

Černý, P.
1989: Exploration strategy and methods for pegmatite deposits of tantalum. *In* Lanthanides, Tantalum, and Niobium. *Edited by* P. Moller, P. Černý and F. Saupe. Springer-Verlag, New York, pages 274-302.

1991a: Rare element granitic pegmatites. Part I: Anatomy and internal evolution of pegmatite deposits. Geoscience Canada, Volume 18, pages 49-67.

1991b. Rare element granitic pegmatites. Part II: Regional and global environments and petrogenesis. Geoscience Canada, Volume 18, pages 68-81.

Černý, P. and Meintzer, R.E.
1988: Fertile granites in the Archean and Proterozoic fields of rare element pegmatites: Crustal environment, geochemistry and petrogenetic relationships. *In* Recent Advances in the Geology of Granite-related Mineral Deposits. Canadian Institute of Mining and Metallurgy, Special Publication 39, pages 170-206.

Colman-Sadd, S.P.
1985: Geology of west part of Great Burnt Lake (12A/8) area. *In* Current Research. Government of Newfoundland and Labrador, Department of Mines and Energy, Mineral Development Division, Report 85-1, pages 105-113.

1986: Geology of the east part of the Snowshoe Pond (12A/7) area. *In* Current Research. Government of Newfoundland and Labrador, Department of Mines and Energy, Mineral Development Division, Report 86-1, pages 179-188.

1987a: Geology of part of the Snowshoe Pond (12A/7) map area. *In* Current Research. Government of Newfoundland and Labrador, Department of Mines and Energy, Mineral Development Division, Report 87-1, pages 297-310.

1987b: Snowshoe Pond, Newfoundland. Government of Newfoundland and Labrador, Department of Mines and Energy, Mineral Development Division, Open File Map 87-87.

1988: Geology of the Snowshoe Pond (12A/7) map area. *In* Current Research. Government of Newfoundland and Labrador, Department of Mines, Mineral Development Division, Report 88-1, pages 127-134.

Colman-Sadd, S.P., Dunning, G.R. and Dec, T.
1992: Dunnage-Gander relationships in central Newfoundland: A sediment provenance and U/Pb age study. American Journal of Science, Volume 292, pages 317-355.

Colman-Sadd, S.P. and Swinden, H.S.
1982: Geology and mineral potential of south-central Newfoundland. Government of Newfoundland and Labrador, Department of Mines and Energy, Mineral Development Division, Report 82-8, 102 pages.

1984: A tectonic window in central Newfoundland? Geological evidence that the Appalachian Dunnage Zone may be allochthonous. Canadian Journal of Earth Sciences, Volume 21, pages 1349-1367.

1989: Cold Spring Pond, Hermitage District, Newfoundland. Map 89-107. Government of Newfoundland and Labrador, Department of Mines, Geological Survey, Open File 12A/01/0531.

Cox, K.G., Bell, J.D. and Pankhurst, R.J.
1979: The Interpretation of Igneous Rocks. Allen and Unwin, London, 450 pages.

Dickson, W.L.
1990: Geology of the North Bay Granite Suite and metasedimentary rocks in southern Newfoundland (NTS 11P/15E, llP/16 and 12A/2E). Government of Newfoundland and Labrador, Department of Mines, Geological Survey, Report 90-3, 101 pages.

Dingwell, D.B., Scarfe, C.M. and Cronin, D.J.
1985: The effect of fluorine on viscosities in the system $Na_2O–Al_2O_3–SiO_2$: Implications for phonolites, trachytes and rhyolites. American Mineralogist, Volume 70, pages 80-87.

Dunning, G.R., O'Brien, S.J., Colman-Sadd, S.P., Blackwood, R.F., Dickson, W.L., O'Neill, P.P. and Krogh, T.E.
1990: Silurian orogeny in the Newfoundland Appalachians. Journal of Geology, Volume 98, pages 895-913.

Evans, D.T.W., Kean, B.F. and Jayasinghe, N.R.
1994a: Geology and mineral occurrences of Noel Pauls Brook. Map 94-222. Government of Newfoundland and Labrador, Department of Mines and Energy, Geological Survey Branch, Open File 12A/09/0685.

Evans, D.T.W., Kean, B.F. and Mercer, N.L.
1994b: Geology and mineral occurrences of Lake Ambrose. Map 94-223. Government of Newfoundland and Labrador, Department of Mines and Energy, Geological Survey Branch, Open File 12A/10/0686.

Frost, B.R. and Frost, C.D.
2008: A geochemical classification for feldspathic igneous rocks. Journal of Petrology, Volume 49, pages 1955-1969.

Jahns, R.H. and Burnham, C.W.
1969: Experimental studies of pegmatite genesis: l. A model for the derivation and crystallization of granitic pegmatites. Economic Geology, Volume 64, pages 843-864.

Jenner, G.A. and Swinden, H.S.
1993: The Pipestone Pond Complex, central Newfoundland: Complex magmatism in an eastern Dunnage Zone ophiolite. Canadian Journal of Earth Sciences, Volume 30, pages 434-448.

Kerr, A.
1997: Space-time composition relationships among Appalachian-cycle plutonic suites in Newfoundland. Geological Society of America, Memoir 191, pages 193-220.

Kerr, A., Jenner, G.A. and Fryer, B.J.
1995: Sm-Nd isotopic geochemistry of Precambrian to Paleozoic granitoid suites and the deep-crustal structure of the southeast margin of the Newfoundland Appalachians. Canadian Journal of Earth Sciences, Volume 32, pages 224-245.

Kerr, A. and McNicoll, V.
2012: New U–Pb geochronological constraints from mineralized granites in southern Newfoundland. In Current Research. Government of Newfoundland and Labrador, Department of Natural Resources, Geological Survey, Report 12-1, pages 21-38.

Linnen, R.L. and Cuney, M.
2005: Granite-related rare-element deposits and experimental constraints on Ta-Nb-W-Sn-Zr-Hf mineralization. In Rare-element Geochemistry and Mineral Deposits. Edited by R.L. Linnen and I.M. Samson. GAC Short Course Notes 17, pages 45-68.

London, D.
2005: Geochemistry of alkali and alkaline earth elements in ore-forming granites, pegmatites and rhyolites. In Rare-element Geochemistry and Mineral Deposits. Edited by R.L. Linnen and I.M. Samson. GAC Short Course Notes 17, pages 17-44.

2016: Rare-element granitic pegmatites. *In* Rare Earth and Critical Elements in Ore Deposits. Society of Economic Geologists, Reviews in Economic Geology, Volume 18, pages 165-193.

Organ, J.S.
2014: Till geochemistry of the Red Indian Lake basin (NTS map areas 12A/04, 5, 6, 7, 9, 10, 11, 15 and 16). Government of Newfoundland and Labrador, Department of Natural Resources, Geological Survey, Open File 012A/1562, 175 pages.

Pearce, J.A., Harris, N.B.W. and Tindle, A.G.
1984: Trace element discrimination diagrams for the tectonic interpretation of granitic rocks. Journal of Petrology, Volume 25, pages 956-983.

Rudnick, R.L. and Gao, S.
2003: Composition of the continental crust. *In* Treatise on Geochemistry (Second Edition), Volume 4, pages 1-51.

Selway, J.B., Breaks, F.W. and Tindle, A.G.
2005: A review of rare-element (Li-Cs-Ta) pegmatite exploration techniques for the Superior Province, Canada, and large worldwide tantalum deposits. Exploration and Mining Geology, Volume 14, pages 1-30.

Shand, S.J.
1922: The problem of the alkaline rocks. Proceedings of the Geological Society of South Africa, Volume 25, pages 19-33.

Smith, J.S., Batterson, M.J. and Taylor, D.M.
2009: Till geochemistry of the south side of the Red Indian Lake basin (NTS map sheets 12A/6, 7, 9, 10, 11, 15 and 16). Government of Newfoundland and Labrador, Department of Natural Resources, Geological Survey, Open File 12A/1449, 152 pages.

Sun, S. and McDonough, W.F.
1989: Chemical and isotopic systematics of oceanic basalts: implications for mantle composition and processes. *In* Magmatism in the Ocean Basins. *Edited by* A.D. Saunders and M.J. Norry. Geological Society of London, Special Publication, Volume 42, pages 313-345.

Swinden, H.S.
1988: Geology of the Pipestone Pond area (12a/1NE, 12A/8E), Newfoundland. Government of Newfoundland and Labrador, Department of Mines, Mineral Development Division, Map 88-051.

Swinden, H.S. and Collins, W.T.
1982: Geology and economic potential of the Great Burnt Lake area, central Newfoundland. *In* Current Research. Government of Newfoundland and Labrador, Department of Mines and Energy, Mineral Development Division, Report 82-1, pages 188-207.

Valverde-Vaquero, P. and van Staal, C.R.
2001: Relationships between the Dunnage-Gander zones in the Victoria Lake-Peter Strides Pond area. *In* Current Research. Government of Newfoundland and Labrador, Department of Mines and Energy, Geological Survey, Report 01-1, pages 159-167.

Valverde-Vaquero, P., van Staal, C.R., McNicoll, V. and Dunning, G.R.
2006: Mid-Late Ordovician magmatism and metamorphism along the Gander margin in central Newfoundland. Journal of the Geological Society, London, Volume 163, pages 347-362.

van der Velden, A.J., van Staal, C.R. and Cook, F.A.
2004: Crustal structure, fossil subduction, and the tectonic evolution of the Newfoundland Appalachians: Evidence from a reprocessed seismic reflection survey. Geological Society of America Bulletin, Volume 116, pages 1485-1498.

van Staal, C.R., Valverde-Vaquero, P., Zagorevski, A., Pehrsson, S., Boutsma, S. and van Noorden, M.J.
2005: Geology, King George IV Lake, Newfoundland and Labrador. Geological Survey of Canada, Open File 1665.

van Staal, C.R., Zagorevski, A., McNicoll, V.J. and Rogers, N.
2014: Time-transgressive salinic and Acadian orogenesis, magmatism and Old Red sandstone sedimentation in Newfoundland. Geoscience Canada, Volume 41(2), pages 138-164.

Whalen, J.B., Currie, K.L. and Chappell, B.W.
1987: A-type granites: geochemical characteristics, discrimination and petrogenesis. Contributions to Mineralogy and Petrology, Volume 95, pages 407-419.

Williams, H., Colman-Sadd, S.P. and Swinden, H.S.
1988: Tectonic-stratigraphic subdivisions of central Newfoundland. *In* Current Research, Part B. Geological Survey of Canada, Eastern and Atlantic Canada, Paper 88-1B, pages 91-98.

Williams-Jones, A.E., Migdisov, A.A. and Samson, I.M.
2012: Hydrothermal mobilisation of the rare earth elements – a tale of "Ceria" and "Yttria". Elements, Volume 8, pages 355-360.

Wilson, M.
1989: Igneous Petrogenesis. Unwin and Hyman, London, 466 pages.

Yu, J.H., O'Reilly, S.Y., Zhao, L., Griffin, W.L., Zhang, M., Zhou, X., Jiang, S.Y., Wang, L.J. and Wang, R.C.
2007: Origin and evolution of topaz-bearing granites from the Nanling Range, South China: A geochemical and Sr–Nd–Hf isotopic study. Mineralogy and Petrology, Volume 90, pages 271-300.